JOURNAL OF GEOPHYSICAL RESEARCH, VOL. 115, D08205, doi:10.1029/2009JD012606, 2010

Chemical ionization mass spectrometric measurements of atmospheric neutral clusters using the cluster-CIMS

Jun Zhao,[1] Fred L. Eisele,[1] Mari Titcombe,[2] Chongai Kuang,[3] and Peter H. McMurry[2]

Received 5 June 2009; revised 9 October 2009; accepted 2 December 2009; published 28 April 2010.

[1] A recently developed chemical ionization mass spectrometer for detecting neutral molecular clusters in the atmosphere (the Cluster-CIMS) is described. This instrument is unique in that it uses a highly sensitive atmospheric chemical ionization technique combined with two neutral cluster separation methods to measure the very low concentrations of clusters formed during nucleation events. This is apparently the first time that selected-ion chemical ionization mass spectrometry has been used to identify nucleating clusters in the atmosphere. The Cluster-CIMS was well calibrated by using an electrospray high-resolution differential mobility analyzer technique, a novel approach to generating and classifying known ion clusters. Field measurements at a moderately polluted urban site and a relatively remote forested site show that the instrument is capable of detecting neutral sulfuric acid clusters (containing up to four sulfuric acid molecules) during relatively strong nucleation events, with a concentration on the order of 10^4 molecular clusters per cubic centimeter at both sites. These measurements also provide evidence that for a given sulfuric acid concentration, the forested site appears to be significantly more efficient at producing sulfate clusters than the urban site is. A comparison between the Cluster-CIMS measurements and the size distribution measurements of nanoparticles demonstrates that the observed nucleation events at the two measurement sites are always associated with high concentrations of sulfuric acid and that, if the clusters are measurable, they are well correlated with the nanoparticles down to ~2 nm; however, other nucleation events are either relatively small or may have occurred prior to reaching the measurement sites, and hence the concentrations of the sulfuric acid clusters are most likely under the detection limit of the Cluster-CIMS. Limitations of the instrument and possible future directions for its development are discussed.

Citation: Zhao, J., F. L. Eisele, M. Titcombe, C. Kuang, and P. H. McMurry (2010), Chemical ionization mass spectrometric measurements of atmospheric neutral clusters using the cluster-CIMS, *J. Geophys. Res.*, *115*, D08205, doi:10.1029/2009JD012606.

1. Introduction

[2] Recent evidence suggests that nanoparticles formed by nucleation grow to sizes large enough to serve as cloud condensation nuclei (CCN) in the course of 1–2 days. Field observations [e.g., *Lihavainen et al.*, 2003; *Kerminen et al.*, 2005; *Laaksonen et al.*, 2005] and models [*Ghan et al.*, 2001; *Spracklen et al.*, 2008; *Kuang et al.*, 2009] have shown that these particles can account for a significant fraction of CCN. The *Intergovernmental Panel for Climate Change* [2007] ranked radiative forcing by aerosols as one of the drivers for climate change, with a total (direct effect plus cloud albedo effect) estimated radiative forcing of -1.2 W cm^{-2}. Locally this could largely compensate for the warming effect caused by various greenhouse gases (CO_2, CH_4, etc). This aerosol effect also represents the largest uncertainty associated with radiative forcing. Although research has been conducted on new particle formation for several decades and much progress has been made, atmospheric nucleation at a microscopic level is still poorly understood. It is commonly recognized that molecular complexes and nucleating clusters are at the initial stage of nanoparticle production. The molecular clusters (effective diameter of ~1 nm) can contain from several to tens of molecules and may exhibit chemical and physical properties strikingly different from those of their bulk counterparts. Knowledge of the chemical composition, concentrations, thermodynamic properties, and evolution of the molecular clusters is required to better elucidate the nucleation process and reduce the uncertainty in the nucleation rates used in global climate models.

[3] Early field measurements showed that sulfuric acid vapor is commonly involved in new particle formation and

[1]Atmospheric Chemistry Division, National Center for Atmospheric Research, Boulder, Colorado, USA.
[2]Department of Mechanical Engineering, University of Minnesota-Twin Cities, Minneapolis, Minnesota, USA.
[3]Department of Chemical Engineering and Materials Science, University of Minnesota-Twin Cities, Minneapolis, Minnesota, USA.

0148-0227/10/2009JD012606

its concentrations are strongly correlated with the production rates of newly formed nanoparticles [*Weber et al.*, 1996, 2001]. Hence, many field studies have attempted to elucidate the nucleation mechanism involving H_2SO_4. Recent field studies have shown that the relationship between the production rate of 1 nm particles, J_1, which is often taken to be a reasonable estimate of the nucleation rate, and sulfuric acid concentration can be empirically expressed as $J_1 = K[H_2SO_4]^P$, where K and P are empirically determined. These studies have consistently found that $1 \le P \le 2$. For measurements carried out in diverse locations ranging from Mexico City to southern oceans, *Kuang et al.* [2008] found that, within experimental uncertainty, $P = 2$ but the prefactor K varies by three orders of magnitude in different locations. *Sihto et al.* [2006] and *Riipinen et al.* [2007] found values of P to be between 1 and 2. The exponent P provides insight into the number of sulfuric acid molecules associated with the critical clusters. Values of 1 and 2 correspond to the activation model [*Kulmala et al.*, 2000, 2006] and to the kinetic model [*McMurry and Friedlander*, 1979; *McMurry*, 1980, 1983] for new particle formation, respectively. The activation model assumes that nucleation occurs through the activation of thermodynamically stable clusters containing one H_2SO_4 molecule, while the kinetic model assumes that critical clusters containing two H_2SO_4 molecules are formed through bimolecular collisions of sulfuric acid. In either model, nucleation may involve other stabilizing molecules as well.

[4] The relative roles of ion-induced and neutral nucleation processes have also been investigated [*Turco et al.*, 1998; *Yu and Turco*, 2000, 2001; *Yu et al.*, 2008]. It is likely that different processes are responsible for nucleation in different regions of the atmosphere. Recent field measurements by *Eisele et al.* [2006] and *Iida et al.* [2006], however, have shown a negligible contribution of ion clusters to new particle formation and growth at one urban and one suburban site, and this has prompted us to focus on the role of neutral clusters in atmospheric nucleation. To date, neutral nucleating clusters have neither been measured directly nor chemically identified due to sensitivity limitations of current instrumentation for measuring atmospheric species at such extremely low concentrations. For a modest-to-strong nucleation event, ultrafine particles (usually larger than 3 nm in diameter) with a concentration of as high as 10^5 cm^{-3} are often observed, and it can be assumed that at least as many precursor clusters (smaller than 1 nm) are produced if coagulation and loss of the clusters to preexisting particles are considered. However, current particle detectors are not capable of detecting these molecular clusters directly. Several condensation particle counters (CPCs) that detect particles as small as 1 nm have been recently developed [*Mordas et al.*, 2005, 2008; *Kulmala et al.*, 2007a; *Laakso et al.*, 2007; *Sipila et al.*, 2008; *Iida*, 2008; *Iida et al.*, 2009; *Lehtipalo et al.*, 2009], but these instruments have lower detection efficiencies dependent on particle size and composition, and they do not discriminate between freshly nucleated clusters and other entities that may undergo condensational growth. In addition, they are unable to provide detailed information on the chemical processes responsible for nucleation. Hereafter, we refer to these nanoparticles detected by CPCs as nanocondensation nuclei (NCN) so as to distinguish them from molecular clusters measured by mass spectrometric technique. *Kulmala et al.* [2007b] reported the existence of atmospheric NCN with a concentration as high as 10^4 cm^{-3}, which is considerably higher than typical concentrations of small ion clusters. However, the NCN concentration was indirectly inferred from the individually measured positive, negative, and total nanoparticle concentrations, which leads to high uncertainty. In principle, mass spectrometry can provide a unique and highly sensitive approach to capturing and chemically identifying molecular clusters ranging in size from individual molecules up to masses of roughly 1000 amu (1.1 nm in diameter, assuming a density of 1 g cm^{-3}) [*Ku and de la Mora*, 2009]. Knowledge of cluster mass would provide constraints on species that participate in the nucleation process, and cluster concentrations would provide information on the kinetics of cluster formation. The challenge with mass spectrometry, however, is that while the total concentration of all clusters might be relatively high, the concentration of a cluster at any particular mass is much lower. Thus, the most abundant individual chemically specific clusters may make up as little as only a few percent of the total cluster concentration, in the range 10^3–10^4 cm^{-3}, close to the detection limit of the current mass spectrometric technique. This makes it very challenging to identify and quantify these atmospheric molecular clusters. Moreover, nucleating clusters may be weakly bound, which also complicates efforts to determine their chemical makeup.

[5] Some nucleating molecular clusters have previously been measured under laboratory experimental conditions [*Eisele and Hanson*, 2000; *Hanson and Eisele*, 2002]. In a laboratory study, sulfuric acid clusters $(H_2SO_4)_n$ (n = 2–8) were generated inside a cooled flow tube at T = 230–260 K and relative humidity (RH) = 20%–65% under elevated sulfuric acid concentration ($1–3 \times 10^9$ cm^{-3}) conditions [*Eisele and Hanson*, 2000]. The cluster ions in the flow tube were formed via two processes: direct ionization of neutral clusters (neutral ionization) and successive ion-molecule clustering processes (ion-induced clustering (IIC)) and then detected with a transverse chemical ionization mass spectrometer. The neutral ionization and IIC may produce the same ion (i.e., the same mass and chemical identity), which the CIMS by itself could not distinguish. However, the neutral ionization can be readily separated from IIC in the transverse drift region of the flow tube on the basis of their different reaction time dependences. The measured neutral cluster distribution provided new insight into the chemical details of the sulfuric acid–water nucleation process, including growth of the clusters up to and above the critical cluster size. It also demonstrated that the general process of new particle formation and early growth can be investigated using the chemical ionization mass spectrometric technique. Other species such as NH_3 or possibly organics might be involved in the nucleation process [*Ball et al.*, 1999; *Zhang et al.*, 2004; *Benson et al.*, 2008, 2009; *Young et al.*, 2008]. In another study, clusters containing both sulfuric acid and ammonia, $(H_2SO_4)_n \cdot (NH_3)_m$ ($2 \le n \le 6$, $0 \le m \le n - 1$), were produced at an even higher temperature (~285 K), much warmer than the binary H_2SO_4–H_2O system required for a detectable concentration of clusters [*Hanson and Eisele*, 2002]. The cluster ions were successfully identified with the same technique, showing its robust potential for unveiling the chemical and physical mechanism for new particle formation and growth. In both studies, concentrations of neutral clusters as high as a few times 10^6 cm^{-3} were estimated.

[6] The laboratory experimental technique has been refined and improved to tackle the far more difficult problem of direct measurement of neutral clusters in the atmosphere, where cluster concentrations are orders of magnitude lower and the ion spectrum is far more complex. The modification and improvement led to recent development of a flow/drift tube chemical ionization mass spectrometer, the Cluster-CIMS. It uses a variable-reaction-time chemical ionization technique, a newly implemented octopole focusing device, and two methods for separating neutral clusters from the IIC process. Recent measurements include those of single molecules as well as their clusters formed during nucleation events and provide mass spectrometric information on their chemical identity up to ~1000 amu. This instrumentation is an outgrowth of the select ion chemical ionization mass spectrometer for measuring trace gases (e.g., sulfuric acid and methane sulfonic acid), which was described by *Eisele and Tanner* [1993], combined with the laboratory techniques discussed above for mass-identifying sulfate clusters [*Eisele and Hanson*, 2000; *Hanson and Eisele*, 2002]. Only those relevant modifications and improvements of the above instruments that enable the measurement of ambient nucleating clusters are discussed here. The Cluster-CIMS we used to carry out the first atmospheric measurements of chemically identified neutral clusters in the atmosphere is described below, followed by our first reported measurements of such clusters in the atmosphere.

2. Experimental Methodology

2.1. Instrumentation

[7] A schematic of the apparatus is presented in Figure 1. Ambient air laden with trace gas molecules and clusters is drawn continuously through a 10 cm ID stainless steel inlet (Figures 1a, 1c, and 1d). A specific species of reactant ions is generated and can be adjusted depending on the chemical nature of the clusters of interest, corresponding to negative and positive ion operation modes. For the purpose of this study, we focused primarily on sulfuric acid and its clusters, using the negative ion operation mode because the negatively charged sulfuric acid clusters are in general more stable than their positively charged counterparts. Ambient air is a chemically complex system, containing both inorganic and organic species, which limits the ions that can be used for chemical ionization. Nitric acid is chosen to generate the primary ions in order to minimize interferences from most air components, thus only allowing clusters with HNO_3 itself or a core ion that is more acidic than HNO_3 to be detected via proton exchange. The primary ions $NO_3^- \cdot (HNO_3)_n$ (n = 1, 2) were produced by introducing trace amounts of HNO_3 from a vial inside a temperature-regulated cooler into a flow of about 2–4 L min^{-1} of pure N_2, which then passed through the ion source (a 1 cm wide by 3 cm long, oval-shaped housing containing a 0.75 mCi radioactive ^{241}Am source). The ratio $[NO_3^- \cdot (HNO_3)_2]/[NO_3^- \cdot HNO_3]$ is controlled to be about 0.1 by adjusting the temperature inside the cooler and the flow rate through the vial so that a controlled amount of HNO_3 vapor is introduced into the ion source. In this way, the primary reactant ion is consistently $NO_3^- \cdot HNO_3$. This reduces the complications from using a wider range of nitrate ions, each of which may react at different reaction rates with sulfuric acid clusters and generate a more complex spectrum.

[8] Laboratory experiments have shown that sulfuric acid clusters up to octamers react efficiently with nitric acid cluster ions [*Eisele and Hanson*, 2000; *Hanson and Eisele*, 2002]. While the use of a reactant ion that excludes the measurement of many either non–sulfate-containing compounds or nonpolar compounds is somewhat restrictive, some type of simplification of the ion spectrum is desirable when exploring this new low-concentration atmospheric molecular cluster regime. Even during a relatively strong nucleation event, the concentration of any nucleation-correlated molecular cluster (e.g., clusters containing three or more sulfuric acid molecules) appears to be only about 1 part per quadrillion by volume (ppqv) or less. While sub-ppqv concentrations of weakly bound chemical clusters are inherently difficult to measure, they are also surrounded by a virtually unexplored sea of other compounds at concentrations that are similar or up to at least three orders of magnitude (1 part per trillion by volume (pptv)) or higher. Many of these compounds appear to have a mass that would suggest a geometrical size up to at least 1 nm in diameter or a mobility size of 1.3 nm or greater [*Ku and de la Mora*, 2009], even though they do not appear to correlate with nucleation events or sulfur plumes; that is, their concentrations do not vary with nanoparticle or SO_2 concentrations, respectively. Note that signals at almost all masses up to 600 greatly exceed counting rates due to electronic background (0.2–0.5 Hz). If this study is initially restricted to observing sulfate-containing clusters, then an upper boundary for the rate of IIC can be obtained, based on the concentration of sulfuric acid. Without such knowledge it is difficult to separate ion-induced processes involving growth compounds present at unknown concentrations from the direct charging of neutral clusters. The separation of large, stable molecules from nucleation-related clusters also becomes more difficult because of the sheer number of compounds and their dynamic changes during the nucleation event that must be considered.

[9] During operation, sampled ambient air that contains molecular clusters and other trace species is drawn into the Cluster-CIMS inlet (Figures 1c and 1d). Reactant ions ($NO_3^- \cdot HNO_3$) formed in the ion source are carried by N_2 into this flow and are electrostatically transported across the flow. Clusters can exchange a proton with the reactant ions in the flow tube, after which the resulting ions/cluster ions are then guided through the inlet by electric fields applied to the tube (Figures 1c and 1d). A very small fraction of flow containing ions is extracted through a 150 μm diameter aperture into the vacuum chamber by the electrostatic field applied on the entrance plate. A dry, pure N_2 buffer gas (~400 cm^3 min^{-1} STP) is injected just before the ions reach the aperture to minimize the water molecules associated with the core ions and also to minimize clustering that can occur as the core ions pass through the supersonic jet expansion (Figure 1b). During this process, the charged H_2SO_4 component is preserved due to the high bonding energy between H_2SO_4 molecules and HSO_4^-; an extreme example is a bonding energy of 42 kcal mol^{-1} for $H_2SO_4 \cdot HSO_4^-$ [*Lovejoy and Curtius*, 2001]. The buffer gas also prevents the ambient fine particles from entering the vacuum system and blocking the aperture. The sampled ions are then guided through a conical octopole

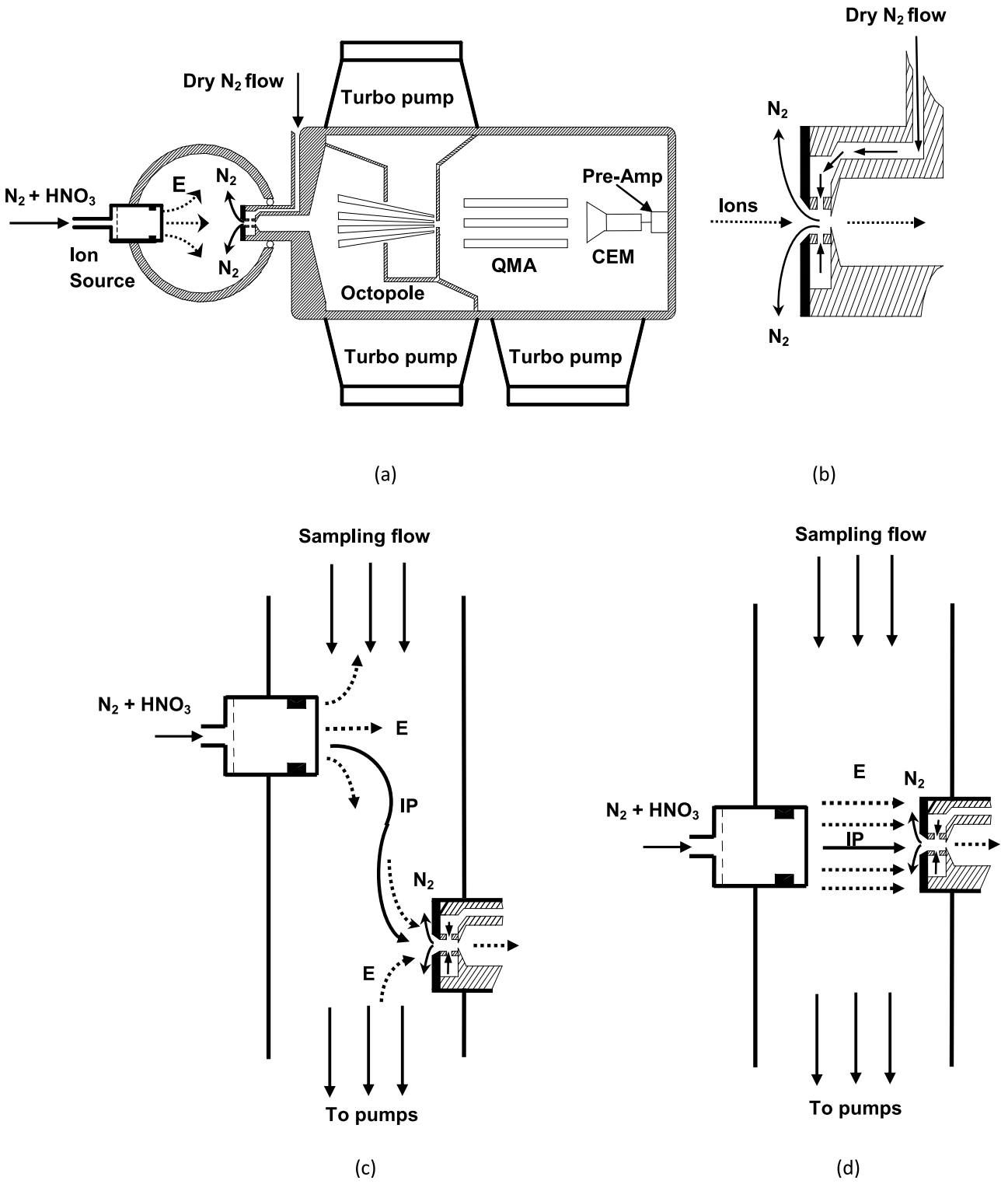

Figure 1. Schematic of the Cluster-CIMS: (a) side view; (b) details of the entrance aperture regime; (c) flow tube operation mode; (d) transverse ion operation mode. CEM, channel electron multiplier; E, electric field; IP, ion path; Octopole, octopole focusing assembly; Pre-Amp, preamplifier; QMA, quadrupole mass analyzer.

device, where they are focused and transported efficiently into the quadrupole mass analyzer region. The use of the conical octopole rather than the collisional dissociation chamber (CDC)-electrostatic lens system is a significant improvement of the Cluster-CIMS compared to previous versions of this instrument when measuring clusters. This change reduces cluster breakup and improves the focusing and transmission efficiency of the ions. The focusing and

transmission of the octopole are sensitive to the frequency and the amplitude applied to it, which can be simulated with ion trajectory software SIMION, as will be described in a separate paper. After leaving the octopole, the ions enter the mass analyzer, which can measure a mass-to-charge ratio (m/z) of up to 1000 amu. This is sufficient for the current application since a mass of 1000 amu (containing 10 H_2SO_4) corresponds to particles (clusters) around 1.1 nm in diameter [*Ku and de la Mora*, 2009], thought to be well above the core size of the critical sulfate clusters in the atmosphere. The cluster-CIMS sensitivity for high-mass clusters was also improved by increasing the accelerating voltage on the cone of the channel electron multiplier (Figure 1a) from 2000 to 3100 V. This helped to accelerate the bigger clusters to higher velocities, thereby making them more efficient electron ejectors when hitting the detector surface, while not significantly increasing the electronic background noise [*Hanson and Eisele*, 2002].

[10] The charging of preexisting neutral clusters (neutral ionization) has a time dependence that is the same for the monomer and all large clusters (sulfuric acid in this case), while the ion-induced molecular clustering process is a sequential process, the clusters containing more molecules having successively higher time dependences. Therefore, by varying the reaction time, one can distinguish the IIC and neutral ionization components [*Eisele and Hanson*, 2000]. In this paper two separate but fairly independent techniques will be used in an attempt to accomplish this separation. The multiple-reaction-time technique previously used in the laboratory [*Eisele and Hanson*, 2000; *Hanson and Eisele*, 2002] can only be applied in a very approximate manner because the atmospheric ion cluster concentrations at the parts per quadrillion by volume level are only slightly above the background levels. The second technique does not require measurements at multiple times but does require some testable assumptions about ion–molecule clustering rates that have not been directly measured. This approach will be discussed in more detail in section 4.

[11] In the multiple-reaction-time technique, reaction times can be varied by either changing the flow velocity in the flow tube for time scales of seconds or changing the voltage applied to the transverse ion source for millisecond scales. We refer to these approaches as the "flow tube" and "transverse" modes, respectively. For the former, the ion source is located ~20 cm upstream of the pinhole aperture, and a reaction time of 0.2–1 s is obtained by changing the flow rates. A direct method has been developed to measure the average reaction time. Initially a positive voltage was applied to the flow tube/ion source so that the negative ions were not emitted from the ion source (i.e., ion source "off mode") and the flow tube/ion source was then rapidly switched to a negative voltage to stimulate the emission of negative ions (i.e., "on mode"). At the same time, the negative ion current delivered to the mass spectrometer was monitored with a digital oscilloscope, which was triggered by the same pulse that turned the ions off and on. The average reaction time is then defined as the time difference between the on-mode pulse and the midpoint in the time-dependent ion collection spectrum. This time difference includes the time during which the ions are transported from the entrance aperture to the detector, but the latter transit time is very short compared to the reaction time. The reaction time is not necessarily proportional to the flow rate since the flow dynamics might change from more laminar flow to more turbulent flow, and the electric field–induced drift velocity plays a more dominant role as flow velocities are reduced. The ion source was redesigned from a previous version [*Eisele and Hanson*, 2000] to allow the pure N_2 to be evenly distributed along the 3 cm long and 1 cm wide ^{241}Am source. This larger, longer, and more aerodynamic source design allows a wider range of flow velocities in the transverse mode and makes available a larger total number of ions in the flow tube mode. It also minimizes direct ionization of ambient air, which can lead to the formation of non-NO_3^- ions (e.g., CO_3^-, CO_4^-). Although the fraction of the latter ions might not be high (likely a few percent) compared to the reactant ions, they may react more efficiently with less acidic trace gases in the air. This could allow the formation of product ions with masses that overlap those of the ions of interest, especially for high flow rate/shorter reaction times. In addition, the ion source housing extends radially into the flow tube and injects nitrogen into the sampled flow, which might disrupt the initially laminar flow (particularly for low flow tube velocities), thus making the flow partially turbulent. In a situation in which the flow tube velocity is very high, the background counts can be dramatically affected because of the more complex ion chemistry resulting from the presence of multiple reactant ions such as CO_3^- and CO_4^- instead of just $NO_3^- \cdot HNO_3$ alone. These other ions are formed because the alpha radiation ionizes some of the air directly in front of the ion source, which for very high flow tube velocities, such as those used in the shortest reaction time measurement, can significantly dilute the HNO_3 concentration (Figure 1c). Hence, care must be taken to choose an appropriate ratio of sample flow/ion source flow to prevent the production of such non-HNO_3 ions.

[12] Alternatively, for the transverse mode, the ion source is located directly ~5 cm across from the entrance plate, while the inlet flow rate is kept constant (Figure 1d). By changing the voltages between the ion source and the plate from −500 to −5000 V, one can obtain an ion-drift time of 3–30 ms, assuming an ion mobility of ~2.0 $cm^2\ V^{-1}\ s^{-1}$ for the cluster ions in air, in a manner similar to that used previously in the laboratory [*Hanson and Eisele*, 2002]. This drift time is the time available for the reaction of primary ions with sulfuric acid and its clusters. In either operation mode, variable reaction time provides a means to distinguish between the ionization of neutral clusters and the IIC process. For typical conditions, the count rate of the reactant ions is around 100 kHz for a 1 s reaction time and up to or greater than 1 MHz for reaction times in the millisecond range, which can lead to detector saturation for the largest peaks. For a cluster concentration of 10^3–10^4 cm^{-3} in the atmosphere during the nucleation event, these clusters are likely under the detection limit of the Cluster-CIMS in the transverse mode. This is primarily due to the more complex spectrum associated with shorter reaction times, where the ions of interest make up a smaller fraction of the total ion concentration. For these reasons, the focus has been on reaction times of 0.2–1 s (i.e., the flow tube mode). The transverse mode might provide more information on dimer concentrations since less ion-induced clustering would occur for the shorter reaction times if high background rates could be avoided. The latter might best be accomplished by using

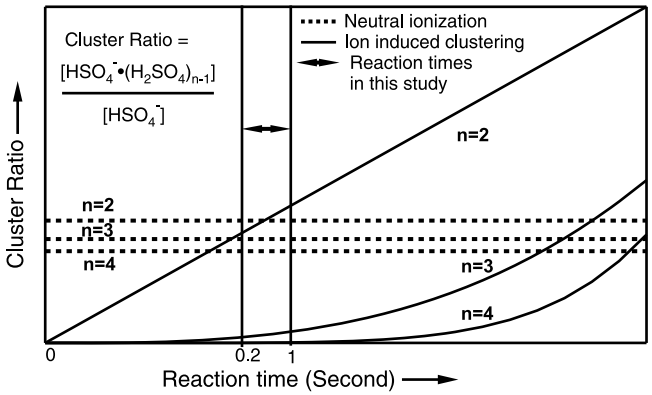

Figure 2. Two competitive processes govern the production of the ion clusters $HSO_4^- \cdot (H_2SO_4)_{n-1}$. The general time dependences of these two processes, ionization of preexisting neutral clusters (dashed lines) and ion-induced clustering (IIC, solid lines), are shown. In each case the process is represented by the ratio of the intensity of the ion clusters ($n \geq 2$) to monomer ($n = 1$). Note that for neutral ionization, the cluster ratio is time independent, while for the IIC process, this ratio can be linear or have higher-order time dependence. The approximate range of reaction times used in this study falls between the two vertical lines.

mass spectrometry/mass spectrometry (MS/MS) or time-of-flight/MS techniques or by choosing a location where the ions observed at mass 195 are nearly exclusively $HSO_4^- \cdot H_2SO_4$.

[13] As stated above, the cluster ions observed in the flow tube originate from one of two processes: neutral ionization or IIC, which have different time dependencies. The time dependence for the ion cluster intensity ($[HSO_4^- \cdot (H_2SO_4)_{n-1}]_t$) divided by the sulfuric acid ion intensity ($[HSO_4^-]_t$) can be expressed as (see Appendix A for details)

$$\frac{[HSO_4^- \cdot (H_2SO_4)_{n-1}]_t}{[HSO_4^-]_t} = a_{n0} + \sum_i^n a_{ni} t^i,\ 1 \leq i \leq n-1 \text{ and } n \geq 2. \quad (1)$$

The first term on the right-hand side of equation (1), a_{n0}, represents ions contributed from ionization of neutral clusters; the second term denotes the IIC process. The a_{ni} is a function of ion-molecular rate constants, the concentrations of the sulfuric acid, and neutral clusters. The $[HSO_4^-]$ represents the intensity of $HSO_4^- \cdot HNO_3$ plus HSO_4^- where the latter is small. The ratio of the higher clusters ($n > 1$) over the sulfuric acid monomer is time independent for neutral ionization but has a linear or higher-order time dependence for the IIC process, and the greater the number of sulfuric acid molecules in the clusters, the greater is the order of the time dependence, as shown in Figure 2. The reaction times used in this study fall within the two vertical lines shown in Figure 2. In this range, IIC dominates over neutral ionization for the dimers, while the IIC contributes negligibly to ion cluster formation for trimers and higher-order clusters for sulfuric acid concentrations measured in these two studies, as will be discussed in the following sections. Nucleating sulfate clusters ($n \leq 4$) with a typical concentration on the order of 10^4 cm^{-3} can typically be measured by the Cluster-CIMS, while larger clusters ($n > 5$) produced from a modest nucleation event are likely out of the detection limit of the present Cluster-CIMS (at least for high-resolution mass measurements).

[14] Note that the $HSO_4^- \cdot (H_2SO_4)_{n-1}$ cluster ions that our present measurements focused on do not include water or other stabilizing components (such as NH_3) since it is hypothesized that those components will fall apart upon ionization or be lost in the vacuum from the core ions $HSO_4^- \cdot (H_2SO_4)_{n-1}$ for small clusters (e.g., $n < 3$–4, particularly for longer reaction times), as discussed by *Hanson and Eisele* [2002] for NH_3. Water molecules readily dissociate upon ionization or in the vacuum because they are weakly bonded to the core sulfuric acid clusters. We have a very limited understanding of what would contribute to the stabilization of the sulfuric acid clusters, and the stabilizing effect of ammonia or other basic or acidic gas-phase compounds for atmospheric clusters is still highly speculative [*Ball et al.*, 1999; *Benson et al.*, 2009; *Kurtén et al.*, 2008; *Zhao et al.*, 2009]. Preliminary laboratory measurement showed that upon adding several parts per billion of NH_3 into the inlet of the Cluster-CIMS with sulfuric acid concentration on the order of 10^9 cm^{-3} (T = 283 K and RH = 30%), mass peaks corresponding to sulfuric acid tetramers and higher-order cluster ions (containing up to 7 H_2SO_4) with one to five ammonia molecules were clearly observed in the flow tube mode (J. Zhao et al., unpublished results, 2009). Recent theoretical calculations imply that although in general the concentrations of amines are typically several orders of magnitude lower than that of ammonia, amines might be more important than ammonia in enhancing neutral sulfuric acid–water nucleation in the atmosphere [*Kurtén et al.*, 2008]. The binding energies for the small amines (containing one to three carbons) with sulfuric acid are in the range 22–30 kcal mol^{-1}, compared to 17 kcal mol^{-1} for ammonia. We can speculate that these amines are attached strongly to sulfuric acid tetramers and higher-order cluster ions and thus can be detected by the Cluster-CIMS. However, if a stabilizing compound, X, were to bond strongly with the clusters and be detected in the form of $HSO_4^- \cdot (H_2SO_4)_{n-1} \cdot X$, one should expect that this ion would be well correlated with the clusters and nanoparticles during the nucleation event. Searching for such a species is in the preliminary stage and will require more full mass spectral scanning, which requires longer scanning time. Searching for X will be the subject of future research. For now, the focus is mainly on the sulfuric acid cluster ions.

2.2. Field Sites

[15] The Cluster-CIMS was deployed for the first time in two studies to test its applicability for measurements of neutral clusters in the atmosphere. The first study was carried out at the Manitou Experimental Forest (MEF) (39°06′N, 105°05′W) during the Southern Rocky Mountains Summer 2008 Study, a component of the Bio-hydro-atmosphere interactions of Energy, Aerosols, Carbon, H_2O, Organics and Nitrogen project. The MEF is located in the foothills of the Rocky Mountains ~45 km northwest of Colorado Springs, Colorado, USA. It has a mean elevation of about 2400 m above sea level, an annual mean temperature of about 5°C, and an annual mean precipitation of about 400 mm. The

vegetation within the experimental forest is dominated by ponderosa pine with a mix of bunchgrasses, forbs, and shrubs. The typical wind pattern consists of light downvalley winds from the south at night, sometimes extending into the day. Light upvalley winds from the north are more common during the day. However, strong winds, when they occur, are nearly always from the west during the day. The site is not heavily impacted by the Front Range urban air masses.

[16] The second study was performed at the Foothill Laboratory of the National Center for Atmospheric Research at Boulder, Colorado, in the fall of 2008. Boulder is a city with a population of about 100,000 just to the east of the Rocky Mountains at an altitude of about 1600 m. The winds usually blow from the west (from the Front Range of the Colorado Rocky Mountains) at night, bringing relatively clean air masses to the measurement site. During the day the winds are more variable, but they typically contain more SO_2 when they blow from the south-southeast. Well-defined SO_2 plumes occasionally intercept the site from a local power plant about 4 km southeast of the site, and broad, less intense plumes can come from Denver, south/southeast of Boulder.

[17] During the two studies, the Cluster-CIMS primarily measured the sulfuric-containing ions/cluster ions along with several adjacent ion masses, in a typical cycle time of 5 min. The measured ions/cluster ions include reagent ions, bisulfate ions, and sulfuric acid cluster ions, and they are assigned different calibration factors according to mass-dependent sensitivities discussed below. These calibration factors are used when calculating ion ratios and neutral cluster concentrations.

3. Mass-Dependent Sensitivity of the Cluster-CIMS

[18] A calibration of mass sensitivity for masses up to 1000 amu is necessary in order to quantitatively estimate the concentration of the observed clusters, as the cluster concentrations are often calculated from the ratios of ion masses for which the detection sensitivity varies greatly. Several factors contribute to the mass-dependent sensitivity of this measurement, including an entrance-aperture mass discrimination factor, an octopole mass-dependent transmission factor, a quadrupole mass-dependent transmission/resolution factor, and a detector mass discrimination factor. The mass resolution is typically adjusted to discriminate an individual mass unit for masses up to ~1000 amu. Thus, the absolute resolution increases approximately linearly with mass. A lower resolution was occasionally used to increase the sensitivity when the atmospheric concentration of masses above 600 amu was extremely low. However, this caused overlap of adjacent masses in the high-mass region.

[19] One controllable variable is the octopole mass-dependent transmission factor. The octopole transmission efficiency is sensitive to the frequency applied to the octopole elements. Calibration performed with various octopole frequencies (from 350 to 750 kHz) over a mass range of 70–700 amu was accomplished by coupling an electrospray to a high-resolution differential mobility analyzer (ES-HDMA) to generate and classify specific mass ions. These ions were then analyzed by either an electrometer or the Cluster-CIMS. Electrospray atomization of ionic solutions has long been applied to produce charged ion droplets in nanometer size ranges [*Rosell-Llompart and de la Mora*, 1994]. The electrospray system used here was similar to the one described by *Ku and de la Mora* [2004]. The organic salt solutions used to produce cluster ions were four tetra-alkyl ammonium halide salts in formamide solution: tetramethyl ammonium iodide (TMAI) (44.8 mM), tetraheptyl ammonium bromide (THAB) (20.0 mM), tetrabutyl ammonium iodide (TBAI) (20.7 mM), and tetrapropyl ammonium iodide (TPAI) (48.4 mM). The test solution was injected into a capillary tube whose sharpened end extends into the electrospray chamber. The solution was then forced into the chamber by a small, slightly pressurized dry N_2 flow, where it mixed with a carrier gas flow of about 5.9 L min^{-1} at the capillary tip. A high voltage was applied to the solution, which was then attracted by an opposite-polarity voltage applied to the chamber, resulting in production of a stable electrospray. Highly disperse positively charged cluster ions in the nanometer size range were thus generated and then transported into an HDMA. The HDMA was previously described by *de Juan and de la Mora* [1998] and *Rosser and de la Mora* [2005]. The HDMA has a larger cross section than traditional DMAs. A high flow rate of sheath gas is pulled through the system to achieve a high Reynolds number (as high as 10^5) while maintaining a laminar flow within the HDMA. These combinations greatly reduce the diffusive broadening in the HDMA and provide a high resolution in the nanometer size range. As the polydisperse cluster ions from the electrospray enter the HDMA, specific cluster ions are identified by scanning a wide range of voltages applied to the HDMA and observing the respective aerosol electrometer signal. The cluster ions of interest are then chosen within a narrow size range by applying a single voltage. The selected narrow range of mobility sizes of ions corresponds to a small range of masses that can then be detected and quantified by the Cluster-CIMS. The cluster ions selected from the ES-HDMA system cover a wide range of masses (70–700 amu), including 74 amu from TMAI, 186 and 499 amu from TPAI, 242 and 611 amu from TBAI, and 410 amu from THAB. The charged clusters correspond to A^+ (i.e., $m/z = 74$, 186, 242, or 410 amu) formed by loss of the halide or $A^+(AB)_1$ (i.e., $m/z =$ 499 and 611 amu) formed by the association of the A^+ ion with the neutral monomer (AB). As mentioned by *Ude and de la Mora* [2005], the irregular shape of HDMAs requires the determination of an instrument constant (k) to relate voltage (V) to mobility (Z), such that $k = ZV/Q$, where Q is the sheath gas flow rate. An instrument constant of 0.0338 cm^{-1} was determined from a sheath flow rate of Q = 782 L min^{-1} for the HDMA, an applied voltage (V) for a specific ion, and the mobility of that ion reported by *Ude and de la Mora* [2005]. Mobilities of 2.0–0.6 cm^2 V^{-1} s^{-1}, corresponding to mobility diameters of 1.0–1.6 nm, were reported by *Ude and de la Mora* [2005] for the use of similar tetra-alkyl ammonium halide salts.

[20] The resulting monodisperse ions from the ES-HDMA were then transported either to the Cluster-CIMS inlet (with the chemical ionization source removed) to identify a mass peak and measure the count rate for these ions or into an electrometer to measure the ion concentration. A metal tube of ~15.25 cm long and 1.25 cm ID, bent at the end, was used to couple the HDMA to the Cluster-CIMS inlet. In this way, the ions could be delivered efficiently to the entrance aperture of the Cluster-CIMS without introducing substantial

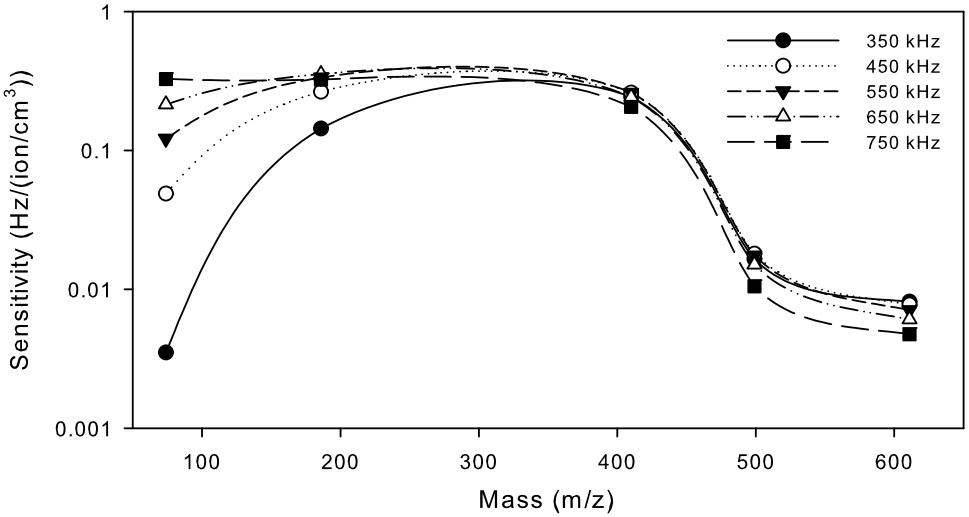

Figure 3. The mass-dependent sensitivity, in Hz $(\text{ion/cm}^3)^{-1}$, of the Cluster-CIMS in the mass range of 70–700 amu at octopole frequencies of 350–750 kHz and for a fixed quadrupole mass resolution of 1 amu (1 amu full width at half maximum).

dilution by an inlet flow of 50–300 L min^{-1} under typical operation conditions. The ions were then extracted into the vacuum system and transported through the octopole and the quadrupole mass analyzer. The count rates of the ions were measured by the Cluster-CIMS with the same mass resolution as the ambient measurements. For a specific mass ion (A^+ or $A^+(AB)_1$), a full mass spectral scanning (from 50 to 700 amu) was also performed to ensure that all the ions are exclusively attributed to the selected mass, and no ions are dissociated in the octopole or the entrance to the vacuum system. Except for the ions from the ES-HDMA system, no other ions were observed, and thus the count rate represents the response of the Cluster-CIMS to a specific mass ion.

[21] As stated above, the count rate of an ion is sensitive to the frequency applied to the octopole. For each ion used in the calibration, the count rate was measured by varying the octopole frequency from 350 to 750 kHz to test the effect of the frequency on the mass sensitivity. Alternatively, the concentrations of the cluster ions exiting the ES-HDMA were measured with an aerosol electrometer (model 3068B, TSI). Ion concentrations are corrected by accounting for the diffusional losses since the transmission efficiencies differ for the straight tube used to transport ions to the electrometer and the bent tube used to deliver ions to the cluster-CIMS. With the count rate measured by the cluster-CIMS and the ion concentration measured by the electrometer, the mass sensitivity (in Hz/(ion cm^{-3})) can be defined as the ratio between the two measurements. The mass sensitivity of the Cluster-CIMS with various octopole frequencies is shown in Figure 3 as a function of mass (Figure 3 does not include m/z = 242 because its ion concentration could not be accurately determined). For the lightest ion, m/z = 74, the sensitivity increased monotonically with octopole frequency, and the sensitivity at 750 kHz can be two orders of magnitude higher than at 350 kHz. For m/z = 186 and above, the octopole frequency has less effect on the sensitivity. For example, for m/z = 186, an octopole frequency greater than 550 kHz does little to improve the sensitivity. In general, the sensitivity decreases slowly from m/z = 186 to 410 and drops rapidly from m/z = 410 to 499. The sensitivity of m/z = 186 is roughly a factor of 2 higher than that of m/z = 410 and is a factor of 20 higher than that of m/z = 499 for an octopole frequency of 550 kHz or lower. The Cluster-CIMS is currently operated with an octopole frequency of 550 kHz, chosen by considering a trade-off for the sensitivity dependence between low mass and high mass. With this frequency, the Cluster-CIMS has similar mass sensitivity (within a factor of 2) for masses between 190 and 410 amu, which cover the masses of the cluster ions containing two to four H_2SO_4. The Cluster-CIMS has sensitivity at least one order of magnitude lower for clusters containing more than five H_2SO_4 than for to smaller clusters, and thus at present it is unlikely to be sensitive enough to measure these larger clusters at high mass resolution. The Cluster-CIMS was previously operated with ~1 MHz octopole frequency, and the mass sensitivity at this frequency was not measured in the calibration. However, we expect that the sensitivity in the mass range of clusters containing two to four H_2SO_4 would be significantly reduced at this frequency relative to a frequency of 550 KHz or lower. Note that the ions used in the calibration are positively charged, while the sulfuric acid clusters measured in the Cluster-CIMS are negatively charged. Positively charged clusters are used in the calibration because they are stable and easily generated, while stable negatively charged clusters in the nanometer size range are currently not well produced by the electrospray atomization. The effect of the charge polarity on the calibration factor is not known, but it is not expected to play a role except possibly for the detector mass discrimination. Here the negative ions were exposed to a slightly higher (10%–25%) accelerating voltage just before impacting the detector. Within the uncertainty of these measurements, it is assumed that a negatively charged cluster has a similar calibration factor to that of a positively charged cluster of equivalent mass. This might need to be further validated.

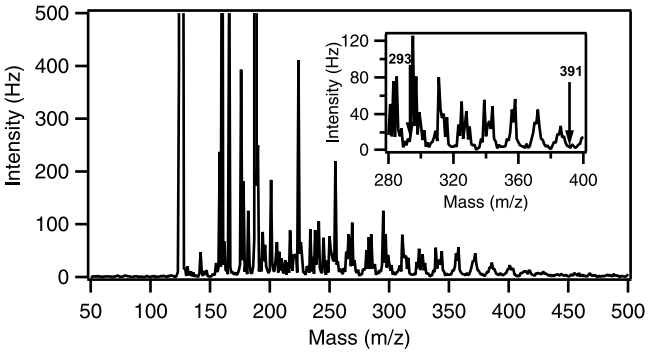

Figure 4. A typical mass spectrum for masses 50–500 amu acquired during a nonnucleation event period at the Boulder site. The inset shows the relative location of masses 293 and 391 compared to other large mass peaks.

More work is needed to produce stable negatively charged clusters in the nanometer size range in order to perform more direct calibrations for negatively charged clusters.

4. Results and Discussion

4.1. Ion Chemistry and Neutral Cluster Concentrations

[22] In order to investigate the ion chemistry and to estimate concentrations of the neutral clusters, we choose two relatively strong nucleation events, on 26 September and 6 August 2008, representing typical characteristics of cluster formation at the Boulder and MEF sites, respectively. The Boulder measurements will be considered first because they involved much higher SO_2 concentrations and better-defined nucleation events. Figure 4 shows a typical mass spectrum measured at the Boulder site when nucleation was not occurring. A somewhat similar spectrum was observed at the MEF. The spectrum is characterized by a series of grouped masses (three or four masses) with an interval of Δm = 14–16 amu above 250 amu. Although this series of masses has not been identified, we can speculate that they are more acidic than HNO_3 or clustered with HNO_3 and may contain $-CH_2-$ (14 amu) or $-O-$ (16 amu) functional groups. A similar but less regular feature was observed at night, suggesting that at least some of these masses are not photooxidation products of volatile organic compounds. These masses might overlap with the nucleation related clusters. Fortunately, as shown in Figure 4, there exists a fairly consistent trough (around 10 masses wide) between these groups. Two of the sulfuric acid clusters (m/z = 293 and 391) are located in the trough, as indicated in the inset in Figure 4. Compared to m/z 391, m/z 293 is closer to a group with dramatic changes in mass peak height. These dramatic changes in the surrounding and possibly overlapping masses will increase the uncertainty of the selected "background level" particularly for m/z 293. Instead, m/z 391 was seen to be closer to the center of another trough, and the adjacent mass peaks are smaller and less variable. Thus, as shown below, there is less uncertainty associated with the background selection for m/z 391.

[23] Full mass spectra were generally not measured when trying to establish the relationship between specific clusters and nucleation events because of the much longer time required to obtain meaningful spectra over a wide mass range. Instead, more integration time was spent measuring parts of the spectrum where sulfuric acid clusters were expected to be observed. In addition to measuring mass peaks thought to be directly related to sulfuric acid clusters, we also measured several masses on either side of these peaks to help ensure that the observed concentration increases in masses 195, 293, and 391 amu during a nucleation event were not some general trend in a larger part of the mass spectrum. The above sulfuric-related peaks generally appeared to be better correlated with the nucleation events than surrounding peaks, although high background and scatter in all masses made this comparison difficult except for the comparison of masses around the mass 195 amu peak.

[24] During a nucleation event, ion concentrations observed at mass 160 amu, $HSO_4^- \cdot HNO_3$, increase substantially and are primarily representative of the sulfuric acid monomer concentration, while those at mass 195 amu correspond to $HSO_4^- \cdot H_2SO_4$, which, as discussed earlier, is potentially derived from the charging of a neutral sulfuric acid dimer plus an ion-induced component. In addition to the ions generated from sulfate compounds, these masses also appear to contain some contribution from other unknown compounds that vary independent of SO_2. In the case of the sulfuric acid monomer and dimer masses, these other compounds make up only a small fraction of the ion concentrations during a nucleation event. For the trimer and tetramer clusters, however, the nonsulfate component can be quite large. Figure 5 shows a plot of the intensities (in hertz) of masses 160 and 195 amu and the SO_2 concentration (in parts per billion) at the Boulder site during a relatively strong nucleation event on 26 September 2008. The abrupt increases and decreases in these concentrations are used to define the time period when sulfuric acid concentration was high and a nucleation event might be expected to occur (as shown between two arrowed lines). Masses 293 and 391 amu, corresponding to the sulfuric acid trimer and tetramer masses, respectively, are also shown in the lower parts of Figure 5. Only a portion of the measured ion concentration at these masses appears to be related to the variation of sulfuric acid and SO_2. The portion of mass 293 and 391 amu signals on either side of the nucleation event in Figure 5 will, for the present purpose, be considered as background. The latter ions represent real but at present unidentified compounds that do not appear to play a role in nucleation. The horizontal lines on either side of the nucleation event correspond to an average of the highest two or three adjacent background points and the average of the lowest two or three background points for each of the two masses. These upper and lower background levels will be used to help bracket the values of the ion concentrations associated with the nucleation event. Figures 5a–5c correspond to ion reaction times of 0.56, 0.37, and 0.17 s, respectively. The upper and lower background count rates are labeled above and under the horizontal lines, respectively. Figure 5d shows the wind direction and speed during the same time period. Note that the wind direction was fairly stable, and the wind speed varied from 1 to 4 mph for a short time before the SO_2 plume intercepted the measurement location; the background concentration was thus probably fairly constant just before and during the event. At the end

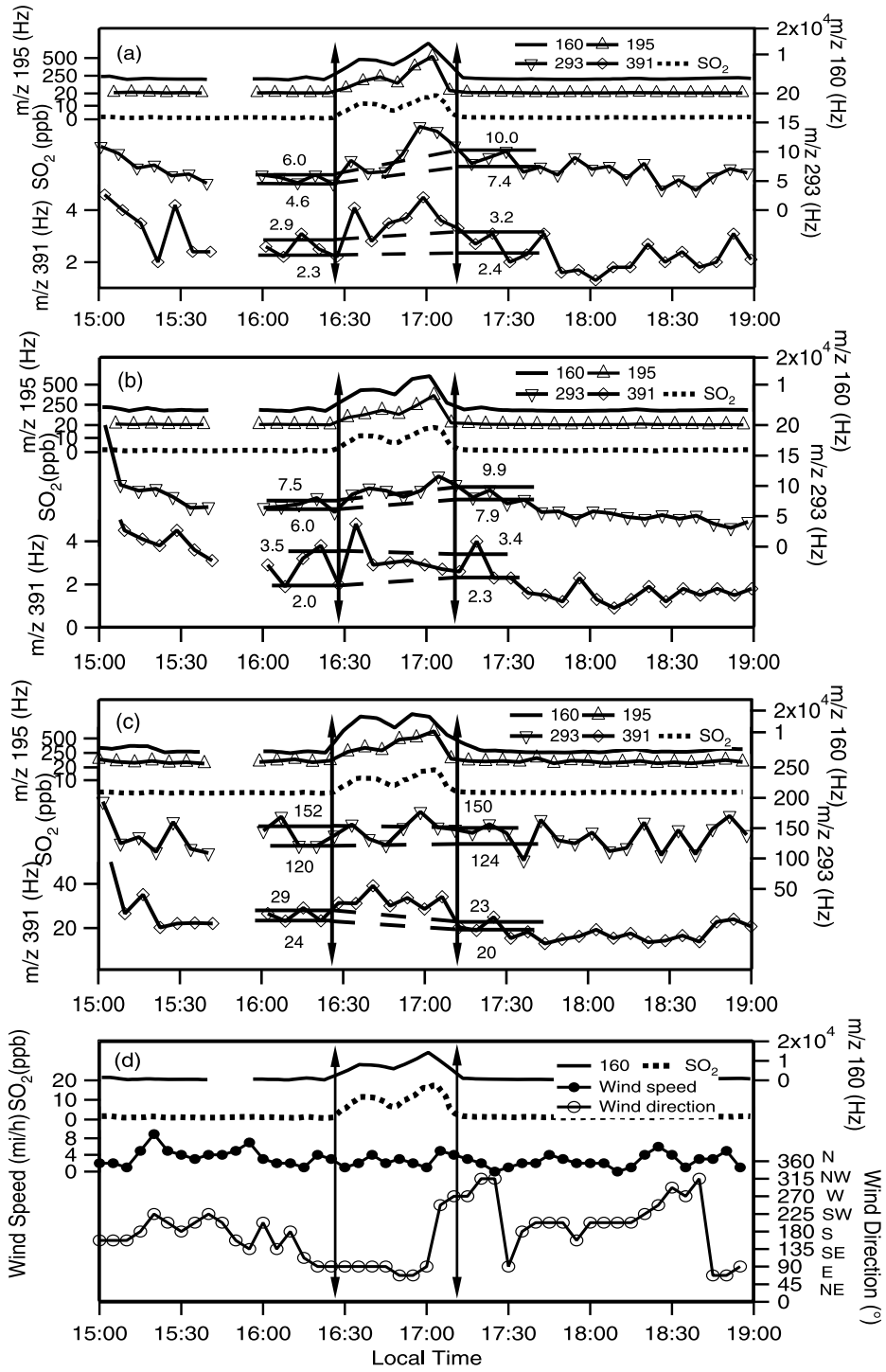

Figure 5. Measurements of masses 160, 195, 293, and 391 along with SO_2 concentration during a nucleation event from 1628 to 1710 LT at the Boulder site on 26 September 2008 for reaction times (a) 0.56 s, (b) 0.37 s, and (c) 0.17 s. The average highest and lowest background count rates just before and after of the event are also shown. (d) Mass 160 and SO_2 concentrations alone shown with wind direction and wind speed for the same time period.

of the event, air masses were not as consistent, but the wind did swing back to the original direction very briefly with no clear difference in background.

[25] Measurements were also made during several events at the MEF. One of the strong events occurred on 6 August 2008 and is shown in Figure 6. Here the spectrum is complicated by the occurrence of a small event at about 1000 LT followed by a stronger event just after 1200 LT. The background just prior to the stronger event, in this case, is sandwiched between two periods of high sulfuric acid

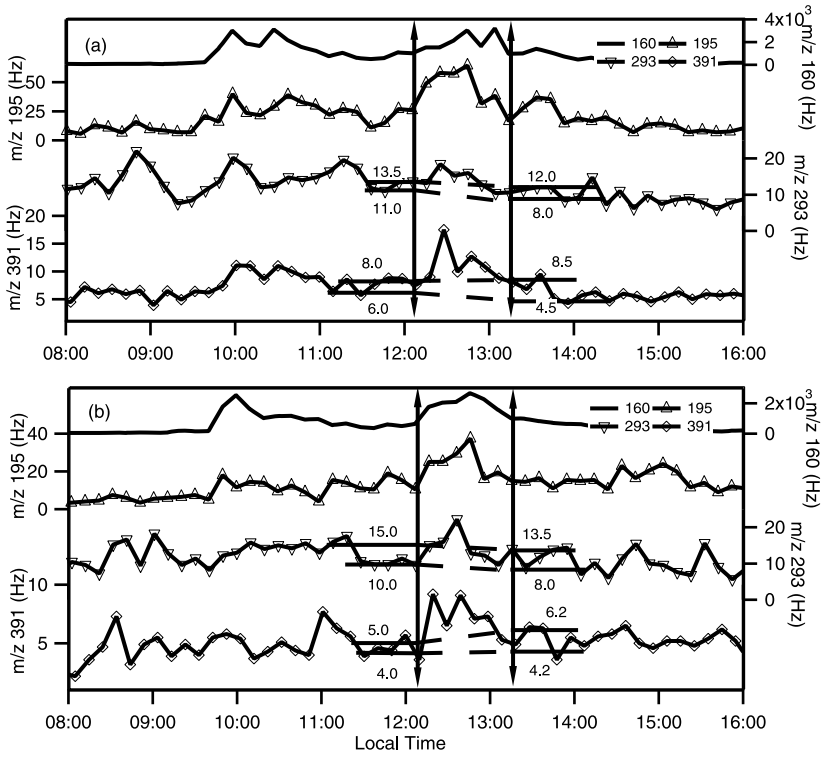

Figure 6. Measurements of masses 160, 195, 293, and 391 during a nucleation event from 1210 to 1320 LT at the Manitou Experimental Forest (MEF) on 6 August 2008 for reaction times (a) 1.42 s and (b) 0.42 s. The average highest and lowest background count rates just before and after the event are also shown.

concentration. Only the stronger event will be considered because signal levels were already close to background levels. Figure 6 again shows a high sulfuric acid event, where the duration of the event is defined by elevated concentrations of masses 160 and 195 amu. Unfortunately, the SO_2 instrument was not functioning properly during the event period, and the meteorological data are also not available for this time period. The concentrations of masses 293 and 391 amu are again small but elevated above background levels during the event time period.

[26] The data from Figures 5 and 6 will be used in two ways to estimate the neutral sulfuric acid trimer and tetramer cluster concentrations. The first approach relies on measurements with multiple reaction times, as discussed in section 2.1. The ratios of total ion count rates for masses 195/160, 293/160, and 391/160 minus the respective upper and lower background count rates for each are plotted as a function of ion–molecule reaction time in Figure 7 for 26 September and in Figure 8 for 6 August. Also plotted in the upper portion of Figures 7 and 8 is an approximate sulfuric acid concentration estimated from the ion ratio of signal minus background for masses 160/125 divided by the reaction time. This also assumes a reaction rate coefficient of 1.9×10^{-9} cm^3 s^{-1} for $NO_3^- \cdot HNO_3 + H_2SO_4$. The dashed and solid lines correspond to the upper and lower limits, respectively, of each cluster ratio, and the distance between these lines corresponds to the measurement uncertainty. As can be seen from Figure 7, there appears to be somewhat of a bias in the sulfuric acid concentration calculated for each of the different reaction times. This is at least in part because of the problem of changing between reaction times either by using different geometries or by changing flow rates. In the future, we expect that this bias can be removed by using a single movable source. At present, the exact reason for these biases is not known, but the shortest reaction time does appear to have significantly higher sulfuric acid concentrations, and the middle time has lower concentrations than the longest measurement time. This bias seems to be reflected also in the time-dependent measurements of each of the masses associated with larger clusters. While the points are quite scattered, there is a clear trend in the mass ratio 195/160 data showing an increase with time. This trend is not seen in the mass ratio 293/160 and 391/160 data, where there might even be a decrease with time. These data are clearly not of the quality measured previously in the laboratory with two orders of magnitude higher cluster concentrations [*Eisele and Hanson*, 2000], but they do show a similar trend, suggesting that ions observed at mass 195 amu might have a significant contribution from IIC, which should result in the 195/160 ion ratio having a positive linear dependence on time. If the *y*-intercept for these ratios could be meaningfully determined, it would represent the ratio of neutral cluster to monomer. The lack of this positive dependence on time for the larger clusters suggests that they are not significantly generated through an ion-induced process. The much higher 293/160 and 391/160 ratios at a 0.17 s reaction time cannot be explained at this time apart from large scatter due to much higher background, but, if they are real, they

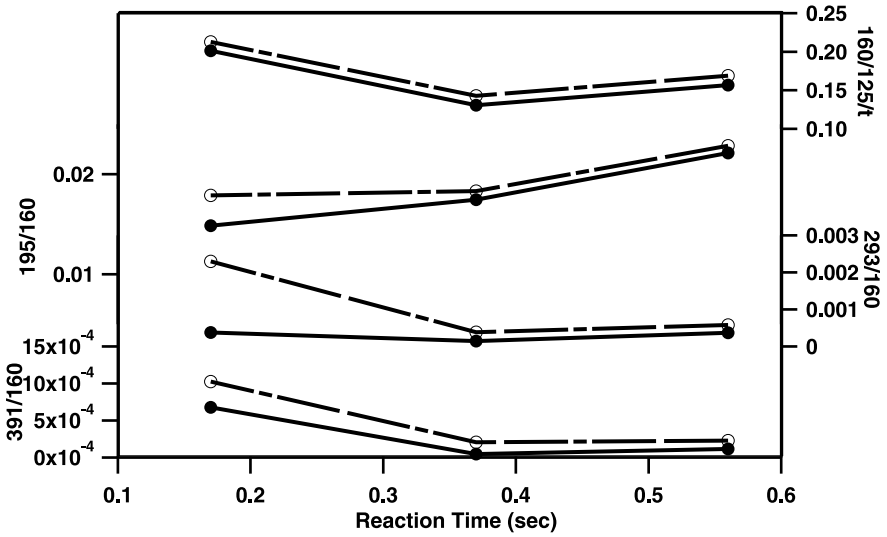

Figure 7. The ratios labeled 195/160, 293/160, and 391/160 are the average counts measured at masses 195, 293, and 391 each divided by the average counts measured at mass 160, respectively, during the nucleation event at the Boulder site on 26 September 2008. The two top lines, 160/125/t, represent approximate sulfuric acid concentration ([160]/[125] per reaction time) for each of the three reaction times. The solid and dashed lines correspond to subtraction of the highest and lowest background levels, respectively, from Figure 5.

are inconsistent with IIC. Figure 8 shows a similar trend for the MEF study, with a somewhat higher estimated sulfuric acid concentration at the shortest reaction time, but still the ratio of masses 195/160 has a positive slope. In this case the 293/160 ratio appears to be approximately time independent but still with a lot of scatter. The ratio of 391/160 also appears to have a positive time dependence but again with a lot of scatter. Although the positive time dependence of 391/160 might show a hint of ion-induced growth, because of the low sulfuric acid concentration and the higher number of sulfuric acid molecules associated with this measurement, it is the least likely, of all of the above, to have a significant ion-induced component. If the ratios of 293/160 and 391/160 were assumed to be time independent, then an approximate estimate of the neutral cluster concentration could be obtained by multiplying each ratio by the appropriate sulfuric acid concentration and averaging the different reaction time values for each cluster size and location. This results in estimated $(H_2SO_4)_3$ and $(H_2SO_4)_4$ concentrations of 3.3×10^4 and 1.9×10^4 cm^{-3} (the shortest reaction times are not included in this estimate), respectively, for the event at Boulder and of 1.3×10^4 and 1.0×10^4 cm^{-3} for that at MEF, respectively.

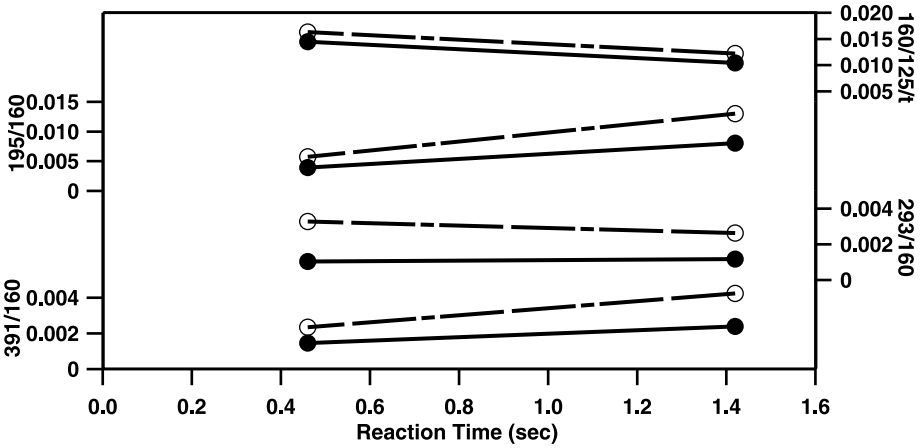

Figure 8. The ratios labeled 195/160, 293/160, and 391/160 are the average counts measured at masses 195, 293, and 391 each divided by the average counts measured at mass 160, respectively, during the nucleation event at the MEF on 6 August 2008. The two top lines, 160/125/t, represent the approximate sulfuric acid concentration ([160]/[125] per reaction time) for each of the two reaction times. The solid lines and dashed lines correspond to the subtraction of the highest and lowest background levels, respectively, from Figure 6.

Although these results are far from conclusive, they do not rely on assumed reaction rates for ion-induced processes to show that neutral clusters are being measured.

[27] The second approach is probably more convincing because it does not rely on trying to extrapolate a line through very scattered points, but it does require some estimates of reaction rate coefficients. This approach simulates the formation of cluster ions using a model based on equation (1). In this case, the ion–molecule rate constants are needed as inputs in order to subtract the calculated ion-induced contribution from the measured ion concentration so that the neutral cluster concentration can be estimated. The formation reactions of a cluster ion $HSO_4^- \cdot (H_2SO_4)_{n-1}$ ($n \geq 2$) include those between neutral clusters $(H_2SO_4)_n$ and the reagent ions (neutral ionization) and between sulfuric acid (H_2SO_4) or neutral clusters $(H_2SO_4)_i$ ($i \leq n-1$) and a cluster ion $HSO_4^- \cdot (H_2SO_4)_{n-2}$ or $HSO_4^- \cdot (H_2SO_4)_{n-i-1}$ (IIC). However, the contribution from the association reactions involving H_2SO_4 is expected to dominate over those involving neutral sulfuric acid clusters since the sulfuric acid concentration is at least several orders of magnitudes higher than those of neutral sulfuric acid clusters.

[28] The rate constants for the reactions of $NO_3^- \cdot (HNO_3)_n$ ($n = 0$–3) with H_2SO_4 have been measured previously using a selected ion flow tube coupled to a chemical ionization mass spectrometer [*Viggiano et al.*, 1997], with a value of 1.86×10^{-9} cm^3 s^{-1} for $NO_3^- \cdot HNO_3$ with H_2SO_4 at 300 K. These measured rate constants (1.7–2.3×10^{-9} cm^3 s^{-1}) are close to the collision-limited rates (1.6–2.2×10^{-9} cm^3 s^{-1}) calculated using the average dipole orientation (ADO) theory [*Su and Bowers*, 1973a, 1973b; *Zhao and Zhang*, 2004] with a dipole moment of 2.8 Debye and a polarizability of 5.4×10^{-24} cm^3 for H_2SO_4. No measured values or theoretical predictions are available in the literature for the rate constants of $NO_3^- \cdot (HNO_3)_n$ with a sulfuric acid dimer or higher-order clusters. A collision-limited rate of 1.9 (2.2) $\times 10^{-9}$ cm^3 s^{-1} for the reaction of $NO_3^- \cdot HNO_3$ with the dimer (trimer) is calculated using the ADO theory based on a dipole moment of 3.4 (4.2) Debye and a polarizability of 11.5 (17.4) $\times 10^{-24}$ cm^3 (F. Yu, State University of New York at Albany, private communication, 2009). A measured rate constant of 1.9×10^{-9} cm^3 s^{-1} for the reaction of sulfuric acid monomer with $NO_3^- \cdot HNO_3$, where $NO_3^- \cdot HNO_3$ is by far the most abundant reactant ion, was adopted, and collision-limited rates of 1.9×10^{-9} and 2.2×10^{-9} cm^3 s^{-1} were used for the reactions of $NO_3^- \cdot HNO_3$ with the dimer and trimer, respectively. A rate constant of 2.2×10^{-9} cm^3 s^{-1} was assumed for the reactions of $NO_3^- \cdot HNO_3$ with the tetramer.

[29] The ion-induced contribution for cluster ions $HSO_4^- \cdot (H_2SO_4)_{n-1}$ ($n \geq 2$) is calculated based on the ion–molecule reaction time, the rate constants for the above-mentioned association reactions, sulfuric acid concentration, and the next-lower-order neutral cluster concentrations (for $n \geq 3$). The sulfuric acid concentration was calculated from the ratio of masses 160/125 divided by the reaction time and the rate constant for reaction between sulfuric acid and the reagent ions, assuming mass 160 to be representative of sulfuric acid. The rate constants for association reactions of sulfuric acid with bisulfate or bisulfate–sulfuric acid clusters have not been measured previously. The association rate constant for $H_2SO_4 + HSO_4^- \rightarrow HSO_4^- \cdot H_2SO_4$ was estimated to be 1.7×10^{-9} cm^3 s^{-1} at 265 K by fitting the signal ratio of ions 195 and 160 versus the ion drift times for the dimers given by *Hanson and Eisele* [2002]. However, this rate coefficient might be overestimated. For the strong nucleation event observed on 26 September 2008, the calculated ion-induced contribution was generally a factor of 2 higher than the measured ion concentration during the nucleation event, assuming an association rate constant of 1.7×10^{-9} cm^3 s^{-1}. This is inconsistent with the idea that mass 195 represents the sum of the charging of neutral dimers and an ion-induced growth component. Therefore, the present results would suggest that an association rate constant of 1.7×10^{-9} cm^3 s^{-1} is at least a factor of 2 too high. Thus an upper limit value for the association rate constant of 8×10^{-10} cm^3 s^{-1} was adopted for the present application. Similarly, for the association reaction $H_2SO_4 + HSO_4^- \cdot H_2SO_4 \rightarrow HSO_4^- \cdot (H_2SO_4)_2$, a comparison between measured ambient ion concentration ratios of the adjacent clusters and predictions from a model based on experimental cluster ion thermodynamics [*Lovejoy et al.*, 2004] was made. The agreement between measurement and model is good only when one-sixth the collision limited rate was used. If the collision-limited rate was used, the model overestimated the ion concentration ratio of $HSO_4^- \cdot (H_2SO_4)_2$ and $HSO_4^- \cdot H_2SO_4$ by a factor of 6. This implies that the association reactions of the bisulfate/sulfuric acid clusters with sulfuric acid may well not proceed at the collision-limited rates, and these reactions might involve a third-body reactant that is not facilitated by ligand switching [*Eisele et al.*, 2006]. For these reasons, a rate coefficient of 3×10^{-10} cm^3 s^{-1} for all the association reactions $H_2SO_4 + HSO_4^- \cdot (H_2SO_4)_{n-1} \rightarrow HSO_4^- \cdot (H_2SO_4)_n$ ($n \geq 2$) was employed in this study, based on a collision rate of 1.5×10^{-9} cm^3 s^{-1} estimated according to the ADO theory.

[30] The above rate constants are incorporated into the model to calculate the neutral cluster concentrations. This estimate is only applied within the chosen nucleation period since the background levels defined above are only valid within these time periods. The actual count rate for each mass is obtained by subtracting the corresponding individual background (each averaged over the highest and lowest background) from the measured count rate when calculating the ion cluster ratio. The neutral fractions for the dimer, trimer and tetramer are obtained by subtracting the ion-induced contribution from the measured ion cluster ratio of masses 195/160, 293/160, and 391/160 respectively. The nucleation periods for the two chosen nucleation events are relatively short (only 1/2 and 1 h for 26 September and 6 August, respectively), which only contain a small number of measurement points. Measurements were made of a large number of masses and several reaction times only about once every 5 min (a little longer for measurements at the MEF). To improve the statistics, cluster concentrations were averaged for the entire nucleation period (concentrations both above and below background levels are included when calculating the averaged neutral cluster concentrations). No dimer concentrations are provided since the association rate constant for the ion-induced reaction for the dimer is forced to a sub–collision-limited rate as discussed above. This treatment results in virtually all the measured ions being produced by IIC for the strong nucleation event (e.g., the one on 26 September). For the less intense event (e.g., the one on 6 August), even the ions observed for the dimer ($m/z = 195$) may contain a contribution from neutral clusters (possibly

Table 1. Estimated Sulfuric Acid and Its Trimer and Tetramer Concentrations on 26 September 2008 in Boulder and 6 August 2008 at the Manitou Experimental Forest[a]

Site and Date	Reaction Time (s)	n = 1 (m/z 160)	n = 3 (m/z 293)	n = 4 (m/z 391)
Boulder, 26 Sep 2008	0.56	9.7×10^7	2.7×10^4	1.3×10^4
	0.37	8.1×10^7	1.2×10^4	6.3×10^3
	0.17	1.2×10^8	9.8×10^4	6.6×10^4
	Average[b]	$8.9(10.0) \times 10^7$	$2.0\ (4.6) \times 10^4$	$9.7\ (26.0) \times 10^3$
Manitou Experimental Forest, 6 Aug 2008	1.42	5.6×10^6	8.3×10^3	1.6×10^4
	0.46	7.5×10^6	1.0×10^4	1.1×10^4
	Average[b]	6.5×10^6	9.3×10^3	1.3×10^4

[a]The values are averaged over the chosen nucleation events for each reaction time. n = 1, 3, and 4 correspond to sulfuric acid monomer, trimer, and tetramer, respectively.
[b]Averaged values are taken over the two longer reaction times. The values in parentheses are averaged over all the three reaction times.

50%). The model calculations show that only a few percent of the measured ions representative of the trimer are ion-induced and virtually all the measured ions are attributed to direct neutral ionization for the tetramer at both sites. Table 1 summarizes the estimated neutral cluster concentrations for the trimer (n = 3) and tetramer (n = 4), along with the monomer sulfuric acid concentration (n = 1) for measurements on 26 September in Boulder and on 6 August at the MEF, respectively. For an averaged sulfuric acid concentration of 9×10^7 cm^{-3} during the nucleation event on 26 September at the Boulder site, the trimer and tetramer concentrations are 2×10^4 and 1×10^4 cm^{-3}, respectively, averaged over the two longer reaction times. Average of 4.6×10^4 and 2.9×10^4 cm^{-3} would be calculated if all three reaction times were averaged (the latter shown in Table 1 in parentheses). While only a slightly higher sulfuric acid concentration was calculated for the shortest reaction time, much higher concentrations were estimated for the trimer and tetramer. As discussed above, much higher "background" levels results in elevated cluster concentrations with higher uncertainty. For an averaged sulfuric acid concentration of 7×10^6 cm^{-3} during the nucleation event on 6 August at the MEF, the estimated trimer and tetramer concentrations were both around 1×10^4 cm^{-3}. To our knowledge, this is the first attempt to estimate atmospheric nucleating cluster concentrations of specific mass clusters during a nucleation event.

[31] The sulfuric acid concentration at the MEF is roughly one order of magnitude lower than at the suburban Boulder site, but it resulted in the production of a similar concentration of trimer and tetramer clusters. *Kuang et al.* [2008] suggested that $J_1 = K[H_2SO_4]^P$, where J_1 is the nucleation rate of 1 nm particles, K is a multiplier that appears to vary with measurement location, and P is typically found to have a value close to 2. For an assumed value of $P = 2$, the value of K is estimated to be 1×10^{-14} and 5×10^{-12} cm^3 s^{-1} for the analyzed nucleation events at Boulder and the MEF, respectively. These prefactor estimates were obtained from nucleation rates calculated according to *Kuang* [2009], accounting for the probability that a nucleated particle will grow to the detection limit using measured aerosol surface areas and growth rates. The K value is a measure of the efficiency with which 1 nm particles or presumably 400–600 amu clusters are produced. A comparison of K values between the MEF and Boulder suggests that the former site is more than two orders of magnitude more efficient than the Boulder site at producing such particles/clusters. Since the average sulfuric acid concentration is a little more than an order of magnitude higher at Boulder than at the MEF, the K value for the production of these clusters would again need to be about two orders of magnitude higher at the MEF than at Boulder, assuming an equal production rate of the specific clusters measured at the two sites. In this case it is not known whether the production rates are similar, only that the cluster concentrations are fairly similar. If cluster growth were only accomplished by the incorporation of sulfuric acid, then it might be expected that a given mass cluster would be lost faster at higher sulfuric acid concentration due to a fast rate of growth to the next-higher cluster, but organics can also play a large role in growth. Coagulation onto larger particles is also a significant loss mechanism for clusters, but neither coagulation nor growth due to organic uptake would be expected to provide loss rates that would differ by an amount even approaching two orders of magnitude. The reasons for far more efficient growth at the MEF are not known. However, it can be expected that any factor favorable to stabilization of the nucleating clusters may accelerate the nucleation process and thus increase the nucleation rate. Since biogenic organic compounds are dominant in the forested sites (e.g., the MEF), it is speculated that organic containing compounds may play a central role in enhancing nucleation rates. More field measurements are needed to elucidate the nucleation mechanisms in different environments.

[32] The concentrations of small (<1 nm) positive and negative ions measured using ion mobility spectrometers (e.g., the inclined grid mobility analyzer (IGMA)) typically range from several hundred per cubic centimeter to 1000 cm^{-3}. The concentrations of neutral clusters measured with the Cluster-CIMS during nucleation are about an order of magnitude higher than these. Condensation particle counters that detect particles as small as 1 nm (i.e., NCN) have recently been deployed for atmospheric measurements, and reported concentrations of the NCN measured with these instruments typically vary between 500 and 50,000 cm^{-3} [*Kulmala et al.*, 2007b; *Lehtipalo et al.*, 2009]. These NCN are, on average, much larger than the sulfuric acid trimer and tetramer measured by the Cluster-CIMS, and they cover a much wider range of sizes. However, the NCN concentrations appear to be roughly of the same order of magnitude as the neutral cluster concentrations measured with the Cluster-CIMS. A more quantitative understanding of these relationships requires further study.

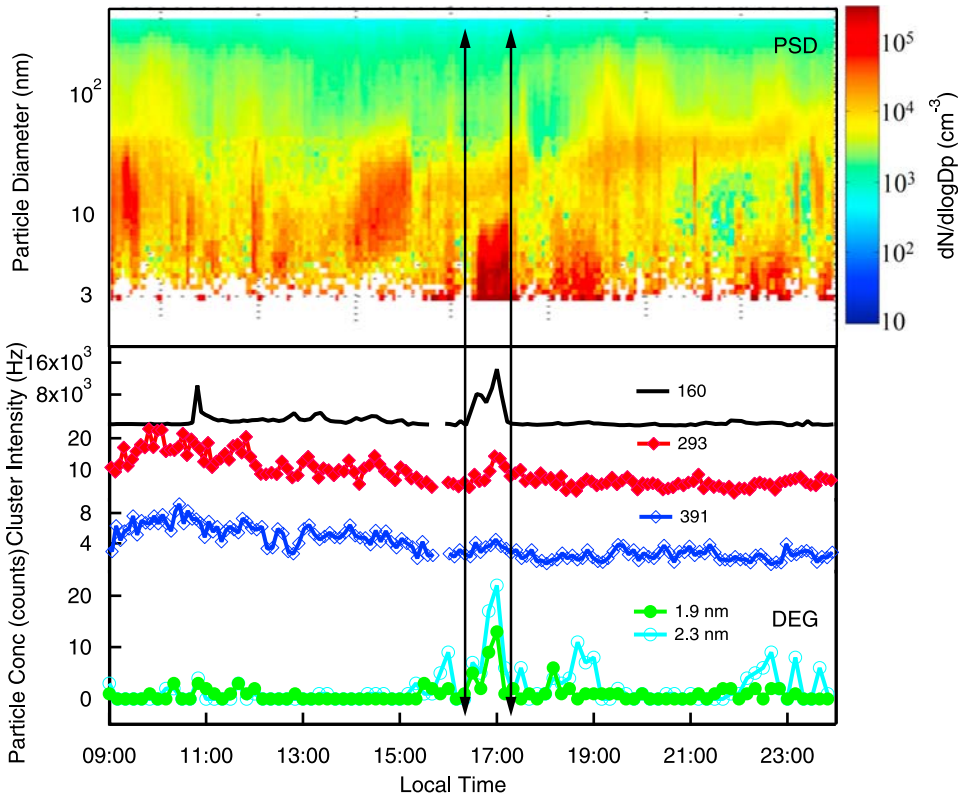

Figure 9. Particle and ion concentrations measured at the Boulder site on 26 September 2008. (top) Measured size distributions of total particles (dN/d log D_p, where dN is the particle concentration and D_p is the particle diameter) (cm^{-3}) in the diameter range 3.0–240 nm from the particle size distribution (PSD) system. (bottom) Measured ion intensities (Hz) corresponding to sulfuric acid (m/z = 160), trimer (m/z = 293), tetramer (m/z = 391), and measured particle counts for two diameter sizes (1.9 and 2.3 nm) from the diethylene glycol (DEG) system. The zone between the two arrowed lines indicates a nucleation event.

4.2. Comparison of Nucleating Clusters and Particle Measurements

[33] Particle sizing and detection instruments, including the particle size distribution (PSD) system (3–4000 nm) and the diethylene glycol (DEG) system (1–15 nm), were also used to measure size distributions of particles simultaneously with the Cluster-CIMS measurements in this study. Detailed descriptions of the PSD system can be found elsewhere [*McMurry et al.*, 2000; *Woo et al.*, 2001; *Iida*, 2008; *Iida et al.*, 2008]. The recently implemented prototype instrument (the DEG system) [*Iida et al.*, 2009] is intended to measure particle sizes down to around 1 nm in diameter. Figure 9 shows size distributions (PSD) and concentrations (DEG) along with ion intensities measured during the nucleation event on 26 September 2008. The abrupt increase and decrease of signal at m/z 160 amu corresponding to sulfuric acid concentrations at ~1630 and ~1710 LT in Figure 9 (bottom) are well correlated with the sharp rise and fall of particle concentrations in Figure 9 (top) in the size range of 3–10 nm measured by the PSD system. The wind direction changed from west to east about 10 min prior to the rise of sulfuric acid concentration and changed back to the northwest 5 min before the end of the event. The changes in the wind direction resulted in different air masses being measured by the instrument, whereas the more easterly wind contained more pollutants from the power plant plume. Abrupt increases of both sulfuric acid and particle concentrations in a short time period are typically indicative of a plume event. The signals corresponding to the trimer and tetramer of sulfuric acid are also seen to vary with sulfuric acid during the nucleation event. The two smallest sizes for which particle concentrations correspond well with sulfuric acid concentrations during the nucleation event are 1.9 and 2.3 nm as measured by the DEG system, as shown in Figure 9 (bottom). The peaks in the concentrations of the 1.9 and 2.3 nm particles at ~1700 LT are consistent with those of sulfuric acid and its trimer and tetramer. The correlation of the particle concentrations (the sum of the two size bins) with sulfuric acid and its trimer and tetramer concentrations during the event show correlation coefficients of 0.80, 0.74, and 0.60, respectively. The particles below 1.9 nm are barely detectable using the DEG system during this nucleation event, probably because of the relatively low detection efficiency of the instrument at such small sizes. The clusters/nanoparticles below this size may suffer more severe diffusional loss in the sampling line of the DEG system than of the Cluster-CIMS. The DEG count rates for particles in the 1.9–2.3 nm range correspond to concentrations of

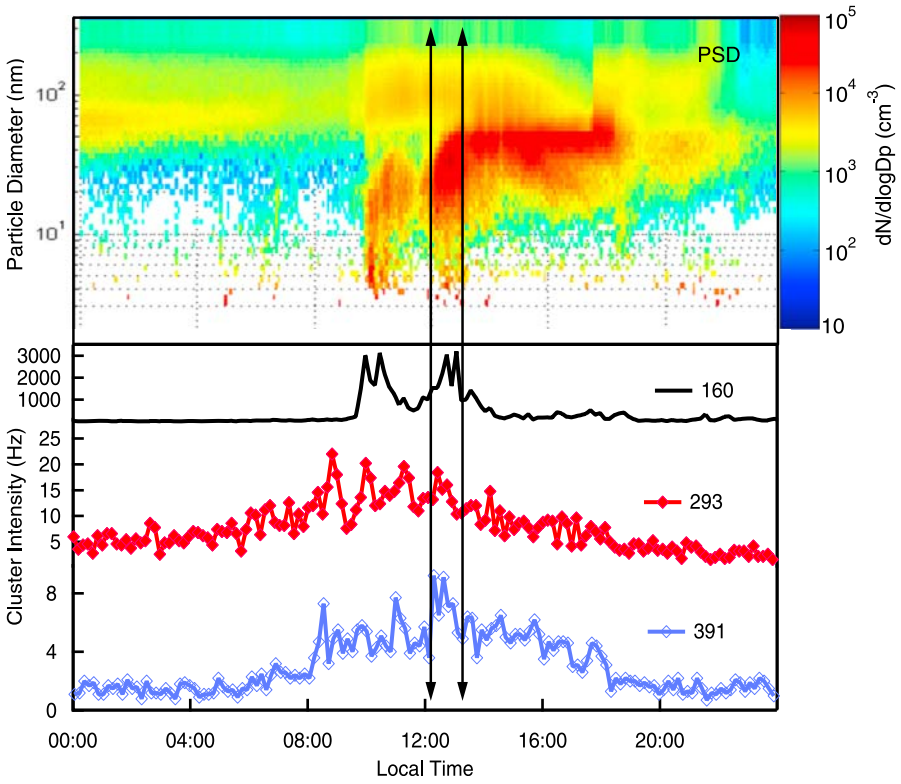

Figure 10. Particle and ion concentrations measured at the MEF on 6 August 2008. (top) Measured size distributions of total particles ($dN/d \log D_p$) (cm^{-3}) in the diameter range 3.0–240 nm from the PSD system. (bottom) Measured ion intensities (Hz) corresponding to sulfuric acid (m/z = 160), trimer (m/z = 293), and tetramer (m/z = 391). The zone between the two arrowed lines indicates a nucleation event.

roughly 10^4 cm^{-3}. Efforts to reduce uncertainties in these measurements and their relationship to the concentrations of smaller mass-selected clusters measured with the Cluster-CIMS are in progress. The combined measurements from the Cluster-CIMS, the DEG system, and the PSD system show that a pool of particles in the size range of 1–10 nm is almost simultaneously detected by the three instruments, as shown in Figure 9. The power plant stack thought to be the origin of the above plume is located around 4 km southeast of the measurement site. It is likely that ultrafine particles in the size range of 1–2 nm are produced continuously in the power plant plume; however, it is unlikely that many of the 1–2 nm particles survive the full trip from the power plant stack to the measurement site. They are probably continuously produced and lost during transport of the plume. The production and loss of the nanoparticles during the transport of a plume from its source to the measurement site will be addressed in a subsequent publication (J. Zhao et al., manuscript in preparation, 2010).

[34] Unlike the plume event shown above, Figure 10 (bottom) shows that the signals at m/z 160, 293, and 391 amu changed more gradually at the beginning and end of the noon nucleation event on 6 August 2008. The trimer and tetramer of sulfuric acid are generally well correlated with sulfuric acid, although there appears to be a smaller nucleation event just prior to noon with relatively large fluctuations in both particles and clusters. Figure 10 (top) shows that particles in the size range 3–10 nm are measured in elevated concentrations in conjunction with higher concentrations of particles in the size range 10–60 nm during the nucleation event. The particles grow continuously after the nucleation event, and concentrations in the size range 20–60 nm stay high into the evening (1900 LT). The characteristics of the event appear to be more regional than plume driven. The smallest size at which the particle concentration shows a good correlation with the event is around 6 nm as measured by the DEG system (not shown in Figure 10). This is not consistent with an estimated concentration of 10^4 cm^{-3} from the Cluster-CIMS measurement, as discussed above. The reason for that is not known. While the DEG system did not detect particles below 6 nm on this particular day, the IGMA [*Tammet*, 2002], which detects and sizes ambient charged particles down to the sub–1 nm range, and the nanoparticle growth system, which detects and sizes neutral particles from 1 to 6 nm, did show evidence for 1–2 nm particle production. The latter instrument, still under development, is based on a concept similar to that behind the pulse height analyzer–ultrafine condensation particle counter [*Saros et al.*, 1996] and is able to detect and size neutral particles through the controlled condensation of oleic acid, a working fluid that has been shown to activate particles as small as 1.2 nm mobility diameter [*Iida et al.*, 2008].

5. Conclusion and Future Perspective

[35] The measurement of nucleating neutral clusters in the atmosphere is extremely difficult due to (1) the complexity

of the spectra arising from the atmospheric ionization of sampled air, even with a highly acidic reagent (e.g., HNO_3); (2) the very low concentration of nucleating neutral clusters (at the parts per quadrillion by volume level or even lower) in the atmosphere; and (3) the difficulty in separating neutral components from ion-induced components. The above points are clearly exemplified by the spectrum in Figure 4, which shows that several of the sulfate peaks expected to play a significant role in nucleation can barely be distinguished from the large number of other, much larger peaks in the mass spectrum. Note also that this spectrum represents only a subset of molecular compounds more acidic than, or clustered with, nitrate ions. Most of the masses seen in Figure 4 show no significant correlation with nucleation or growth events, and many are present most of the time. Some may be clusters, but many are not easily dissociated and may simply be large organic complexes. Most of this spectrum, particularly at the higher mass range, is unexplored, and even the largest peaks above mass 250 amu could correspond to neutral concentrations below 1 pptv. Thus, the atmosphere typically appears to have a relatively large number of different compounds with a geometric size on the order of 1 nm diameter. In spite of their fairly large size, it is not clear that these compounds have any relation to particle nucleation. These massive compounds are, however, a largely untapped source of information on complex atmospheric emissions and their reaction products.

[36] In this first attempt to measure these extremely low concentrations of nucleating clusters, several insights were gained. While absolute sensitivity is important, the ability to distinguish between compounds that are associated with nucleation and those that are not is equally critical to identifying nucleating neutral clusters. Measurements of mass alone are not always sufficient to distinguish these nucleating clusters because of the complexity of the observed spectra, which often have many overlapping mass peaks. Also, temporal correlation with observed nucleation events, particularly those that are regional in origin, has only limited value because of the many ongoing chemical changes observed, even in relatively uniform air masses. In addition, many nucleation events are observed during air mass changes. Thus, a combination of correlations between known aerosol precursors as well as nucleation events and changes in wind directions are beneficial. A calibration that allows the detection sensitivity for various sizes of mass clusters to be directly compared to each other also provides a means for identifying specific cluster growth channels. The present results show the concentrations of trimers and tetramers to be quite similar to each other, which is to be expected if the critical cluster contains fewer than three H_2SO_4.

[37] In addition, the ability to distinguish IIC from the charging of preexisting neutral clusters is critical to identifying nucleating neutral clusters, particularly in the smallest size ranges. Progress on several of these fronts has made possible the measurement of the nucleating clusters in this set of studies. Recent field measurements at a suburban site (Boulder) and a ponderosa pine forest site (MEF) show that the Cluster-CIMS can measure neutral clusters containing three or four H_2SO_4 at concentrations on the order of 10^4 cm^{-3} for relatively strong nucleation events. Since several of these cluster masses might be included in the measurement of 1.0 ± 0.2 nm diameter particles, total cluster concentrations of 10^5 cm^{-3} might be expected for relatively strong nucleation events.

[38] The measurements show that although sulfuric acid concentration in the forested Manitou site is generally one order of magnitude lower than that at the Boulder site, a similar order of magnitude of concentrations of clusters (10^4 cm^{-3}) containing three or four H_2SO_4 are observed for both sites. The prefactor K given by *Kuang et al.* [2008] is an indication of nucleation efficiency in the sense that the higher the K, the more efficient the nucleation (i.e., more nuclei are formed) for a given amount of sulfuric acid. Although the present measurements are still somewhat crude, the K value estimated at the MEF was about two orders of magnitude higher than that observed at the Boulder city site. The greater efficiency of nucleation at the MEF suggests that biogenic emitted organics may play an important role in enhancing nucleation rates.

[39] The current Cluster-CIMS is subject to significant interference from nonsulfuric compounds, which are present much of the time and have masses similar to those being studied but do not correlate with nucleation events. In an attempt to alleviate this problem, in the near future an MS/MS technique will be used to supplement the present technique, providing additional insight into the speciation of these nucleation-related masses and better establishing the identity of sulfate and related peaks. The MS/MS should also largely remove what is presently referred to as background counts; that is, daughter ion spectra should allow sulfuric acid–based ions at mass 293 and 391 amu to be separated from ions that are not sulfuric based. In addition, reaction times at present are varied either by changing between two ion source locations with different geometries while keeping the inlet flow constant or changing the flow velocity while using a fixed ion source geometry in one location. In either case, the flow dynamics and hence the ion chemistry inside the inlet are affected slightly differently for each different reaction time. In the future a single movable ion source will be used to vary reaction times instead of changing flow rates or switching between ion sources with slightly different geometries.

Appendix A

[40] The formation of the bisulfate/bisulfate-nitric acid cluster ions and the sulfuric acid cluster ions is governed by the following reactions (shown only up to tetramer for the current application; for simplicity, nitric acid is not shown in the reactions; e.g., $NO_3^- \cdot HNO_3$ and $HSO_4^- \cdot HNO_3$ are denoted $NO_3^-$and HSO_4^-, respectively):

$$\text{(R1)} \qquad H_2SO_4 + NO_3^- \xrightarrow{k_1} HSO_4^- + HNO_3,$$

$$\text{(R2)} \qquad (H_2SO_4)_n + NO_3^- \xrightarrow{k_n} HSO_4^- \cdot (H_2SO_4)_{n-1} + HNO_3,$$

$$\text{(R3)} \qquad (H_2SO_4)_i + HSO_4^- \cdot (H_2SO_4)_{n-i-1} \xrightarrow{k_{ni}} HSO_4^- \cdot (H_2SO_4)_{n-1},$$

where $1 \le i \le n - 1$ and $2 \le n \le 4$.

[41] The sulfuric acid monomer was represented by bisulfate–nitric acid cluster ion (mass 160 amu, reaction (R1)). For dimer and bigger clusters, their corresponding ions are formed via the neutral ionization (reaction (R2)) and ion-induced clustering (IIC) (reaction (R3)). The ion molecule rate constants are discussed in more detail in section 4. Using a method similar to that described by *Hanson and Eisele* [2002], we can derive the time-dependent ratios of masses 195/160, 293/160, and 391/160 as follows:

$$\frac{[HSO_4^- \cdot (H_2SO_4)_{n-1}]_t}{[HSO_4^-]_t} = a_{n0} + \sum_i^n a_{ni} t^i,\ 1 \le i \le n-1 \text{ and } n \ge 2, \tag{A1}$$

where

$$a_{n0} = \frac{k_n}{k_1}\left(\frac{[(H_2SO_4)_n]}{[H_2SO_4]}\right)$$

$$a_{21} = \frac{k_{21}}{2}[H_2SO_4]$$

$$a_{31} = \frac{1}{2}(k_{31}+k_{32})\frac{k_3}{k_1}[(H_2SO_4)_2]$$

$$a_{32} = \frac{k_{21}k_{31}}{6}[H_2SO_4]^2$$

$$a_{41} = \frac{1}{2}\left(\frac{k_3k_{41}}{k_1}[(H_2SO_4)_3] + \frac{k_2k_{42}}{k_1}[(H_2SO_4)_2]^2 + k_{43}[(H_2SO_4)_3]\right)$$

$$a_{42} = \frac{1}{6}\left(k_{21}k_{42} + k_{43}\left(k_{32} + \frac{k_2k_{31}}{k_1}\right)\right)[(H_2SO_4)_2][H_2SO_4]$$

$$a_{43} = \frac{k_{21}k_{31}k_{41}}{24}[H_2SO_4]^3.$$

[42] Equation (A1) includes both time-independent and time-dependent components, corresponding to neutral cluster ionization and the ion-induced clustering. The ratios shown above are corrected by different calibration factors (see Figure 3) when estimating the neutral cluster concentrations. Because the sulfuric acid concentration is usually several orders of magnitude higher than concentrations of the dimer and higher-order clusters, the contribution from the reactions involving sulfuric acid usually dominates over those involving neutral clusters for the ion-induced clustering process. Also, ammonia is not included in the model reactions. As pointed out in laboratory studies by *Hanson and Eisele* [2002], the dimer and trimer ions, along with the NH_3 presumably associated with these neutral species, had a limited survival time after charging. The present measurements are about two orders of magnitude longer, so their survival lifetimes are even shorter. For the tetramer and above, no apparent correlation between the peaks corresponding to the ammonia clusters and sulfuric acid clusters was observed, but only a limited amount of time was spent searching for these peaks in the present study.

[43] **Acknowledgments.** This work was funded by NSF award ATM-0506674. PHM was supported by a Guggenheim Fellowship. The authors acknowledge Fangqun Yu for providing the calculated dipole moments and polarizabilities of the dimer and trimer of sulfuric acid. Initial help with the Cluster-CIMS operation from Jeff Rathbone is gratefully acknowledged. The National Center for Atmospheric Research is sponsored by the National Science Foundation. Any opinions, findings, and conclusions or recommendations expressed in the publication are those of the authors and do not necessarily reflect the views of the National Science Foundation. We acknowledge the reviewers for valuable comments.

References

Ball, S. M., D. R. Hanson, F. L. Eisele, and P. H. McMurry (1999), Laboratory studies of particle nucleation: Initial results for H_2SO_4, H_2O, and NH_3 vapors, *J. Geophys. Res.*, *104*(D19), 23,709–23,718.

Benson, D. R., L. H. Young, F. R. Kameel, and S. H. Lee (2008), Laboratory-measured nucleation rates of sulfuric acid and water binary homogeneous nucleation from the SO_2+OH reaction, *Geophys. Res. Lett.*, *35*(11), L11800, doi:10.1029/2008GL033387.

Benson, D. R., M. E. Erupe, and S. H. Lee (2009), Laboratory-measured H_2SO_4-H_2O-NH_3 ternary homogeneous nucleation rates: Initial observations, *Geophys. Res. Lett.*, *36*, L15818, doi:10.1029/2009GL038728.

de Juan, L., and J. F. de la Mora (1998), High resolution size analysis of nanoparticles and ions: Running a Vienna DMA of near optimal length at Reynolds numbers up to 5000, *J. Aerosol Sci.*, *29*(5–6), 617–626, doi:10.1016/S0021-8502(97)10028-3.

Eisele, F. L., and D. R. Hanson (2000), First measurement of prenucleation molecular clusters, *J. Phys. Chem. A*, *104*(4), 830–836, doi:10.1021/jp9930651.

Eisele, F. L., and D. J. Tanner (1993), Measurement of the gas-phase concentration of H_2SO_4 and methane sulfonic acid and estimates of H_2SO_4 production and loss in the atmosphere, *J. Geophys. Res.*, *98*(D5), 9001–9010.

Eisele, F. L., E. R. Lovejoy, E. Kosciuch, K. F. Moore, R. L. Mauldin, J. N. Smith, P. H. McMurry, and K. Iida (2006), Negative atmospheric ions and their potential role in ion-induced nucleation, *J. Geophys. Res.*, *111*(D4), D04305, doi:10.1029/2005jd006568.

Ghan, S. J., R. C. Easter, E. G. Chapman, H. Abdul-Razzak, Y. Zhang, L. R. Leung, N. S. Laulainen, R. D. Saylor, and R. A. Zaveri (2001), A physically based estimate of radiative forcing by anthropogenic sulfate aerosol, *J. Geophys. Res.*, *106*(D6), 5279–5293.

Hanson, D. R., and F. L. Eisele (2002), Measurement of prenucleation molecular clusters in the NH_3, H_2SO_4, H_2O system, *J. Geophys. Res.*, *107*(D12), 4158, doi:10.1029/2001jd001100.

Iida, K. (2008), Atmospheric nucleation: Development and application of nanoparticle measurements to assess the roles of ion-induced and neutral processes, Ph.D. dissertation, Univ. of Minnesota, Minneapolis.

Iida, K., M. Stolzenburg, P. McMurry, M. J. Dunn, J. N. Smith, F. Eisele, and P. Keady (2006), Contribution of ion-induced nucleation to new particle formation: Methodology and its application to atmospheric observations in Boulder, Colorado, *J. Geophys. Res.*, *111*, D23201, doi:10.1029/2006JD007167.

Iida, K., et al. (2008), An ultrafine, water-based condensation particle counter and its evaluation under field conditions, *Aerosol Sci. Technol.*, *42*(10), 862–871, doi:10.1080/02786820802339579.

Iida, K., M. R. Stolzenburg, and P. H. McMurry (2009), Effect of working fluid on sub–2 nm particle detection with a laminar flow ultrafine condensation particle counter, *Aerosol Sci. Technol.*, *43*(1), 81–96, doi:10.1080/02786820802488194.

Intergovernmental Panel on Climate Change (2007), *Climate Change 2007: The Physical Science Basis. Contribution of Working Group I to the Fourth Assessment Report of the Intergovernmental Panel on Climate Change*, edited by S. Solomon et al., 996 pp., Cambridge Univ. Press, New York.

Kerminen, V. M., H. Lihavainen, M. Komppula, Y. Viisanen, and M. Kulmala (2005), Direct observational evidence linking atmospheric aerosol formation and cloud droplet activation, *Geophys. Res. Lett.*, *32*(14), L14803, doi:10.1029/2005GL023130.

Ku, B. K., and J. F. de la Mora (2004), Cluster ion formation in electrosprays of acetonitrile seeded with ionic liquids, *J. Phys. Chem. B*, *108*(39), 14915–14923, doi:10.1021/jp0401933.

Ku, B. K., and J. F. de la Mora (2009), Relation between electrical mobility, mass, and size for nanodrops 1–6.5 nm in diameter in air, *Aerosol Sci. Technol.*, *43*(3), 241–249, doi:10.1080/02786820802590510.

Kuang, C. (2009), Atmospheric nucleation: Measurements, mechanisms, and dynamics, Ph.D. dissertation, Univ. of Minnesota, Minneapolis.

Kuang, C., P. H. McMurry, A. V. McCormick, and F. L. Eisele (2008), Dependence of nucleation rates on sulfuric acid vapor concentration in diverse atmospheric locations, *J. Geophys. Res. Atmosphere*, *113*(D10), D10209, doi:10.1029/2007jd009253.

Kuang, C., P. H. McMurry, and A. V. McCormick (2009), Determination of cloud condensation nuclei production from measured new particle formation events, *Geophys. Res. Lett.*, *36*, L09822, doi:10.1029/2009GL037584.

Kulmala, M., U. Pirjola, and J. M. Makela (2000), Stable sulphate clusters as a source of new atmospheric particles, *Nature*, *404*(6773), 66–69, doi:10.1038/35003550.

Kulmala, M., K. E. J. Lehtinen, and A. Laaksonen (2006), Cluster activation theory as an explanation of the linear dependence between formation rate of 3 nm particles and sulphuric acid concentration, *Atmos. Chem. Phys.*, *6*(3), 787–793.

Kulmala, M., et al. (2007a), The condensation particle counter battery (CPCB): A new tool to investigate the activation properties of nanoparticles, *J. Aerosol Sci.*, *38*(3), 289–304, doi:10.1016/j.jaerosci.2006.11.008.

Kulmala, M., et al. (2007b), Toward direct measurement of atmospheric nucleation, *Science*, *318*(5847), 89–92, doi:10.1126/science.1144124.

Kurtén, T., V. Loukonen, H. Vehkamaki, and M. Kulmala (2008), Amines are likely to enhance neutral and ion-induced sulfuric acid–water nucleation in the atmosphere more effectively than ammonia, *Atmos. Chem. Phys.*, *8*(14), 4095–4103.

Laakso, L., S. Gagne, T. Petaja, A. Hirsikko, P. P. Aalto, M. Kulmala, and V. M. Kerminen (2007), Detecting charging state of ultra-fine particles: Instrumental development and ambient measurements, *Atmos. Chem. Phys.*, *7*(5), 1333–1345.

Laaksonen, A., A. Hamed, J. Joutsensaari, L. Hiltunen, F. Cavalli, W. Junkermann, A. Asmi, S. Fuzzi, and M. C. Facchini (2005), Cloud condensation nucleus production from nucleation events at a highly polluted region, *Geophys. Res. Lett.*, *32*(6), L06812, doi:10.1029/2004GL022092.

Lehtipalo, K., M. Sipilä, I. Riipinen, T. Nieminen, and M. Kulmala (2009), Analysis of atmospheric neutral and charged molecular clusters in boreal forest using pulse-height CPC, *Atmos. Chem. Phys.*, *9*(12), 4177–4184.

Lihavainen, H., V. M. Kerminen, M. Komppula, J. Hatakka, V. Aaltonen, M. Kulmala, and Y. Viisanen (2003), Production of "potential" cloud condensation nuclei associated with atmospheric new-particle formation in northern Finland, *J. Geophys. Res.*, *108*(D24), 4782, doi:10.1029/2003jd003887.

Lovejoy, E. R., and J. Curtius (2001), Cluster ion thermal decomposition (II): Master equation modeling in the low-pressure limit and fall-off regions. Bond energies for $HSO_4^-(H_2SO_4)_x(HNO_3)_y$, *J. Phys. Chem. A*, *105*(48), 10874–10883, doi:10.1021/jp012496s.

Lovejoy, E. R., J. Curtius, and K. D. Froyd (2004), Atmospheric ion-induced nucleation of sulfuric acid and water, *J. Geophys. Res.*, *109*(D8), D08204, doi:10.1029/2003jd004460.

McMurry, P. H. (1980), Photochemical aerosol formation from SO_2: A theoretical-analysis of smog chamber data, *J. Colloid Interface Sci.*, *78*(2), 513–527, doi:10.1016/0021-9797(80)90589-5.

McMurry, P. H. (1983), New particle formation in the presence of an aerosol-rates, time scales, and sub–0.01 micron meter size distributions, *J. Colloid Interface Sci.*, *95*(1), 72–80, doi:10.1016/0021-9797(83)90073-5.

McMurry, P. H., and S. K. Friedlander (1979), New particle formation in the presence of an aerosol, *Atmos. Environ.*, *13*(12), 1635–1651, doi:10.1016/0004-6981(79)90322-6.

McMurry, P. H., K. S. Woo, R. Weber, D. R. Chen, and D. Y. H. Pui (2000), Size distributions of 3–10 nm atmospheric particles: Implications for nucleation mechanisms, *Philos. Trans. R. Soc. Lond. Ser. A Math. Phys. Eng. Sci.*, *358*(1775), 2625–2642.

Mordas, G., M. Kulmala, T. Petaja, P. P. Aalto, V. Matulevicius, V. Grigoraitis, V. Ulevicius, V. Grauslys, A. Ukkonen, and K. Hameri (2005), Design and performance characteristics of a condensation particle counter UF-02proto, *Boreal Environ. Res.*, *10*(6), 543–552.

Mordas, G., M. Sipila, and M. Kulmala (2008), Nanometer particle detection by the condensation particle counter UF-02proto, *Aerosol Sci. Technol.*, *42*(7), 521–527, doi:10.1080/02786820802220233.

Riipinen, I., et al. (2007), Connections between atmospheric sulphuric acid and new particle formation during QUEST III–IV campaigns in Heidelberg and Hyyti, *Atmos. Chem. Phys.*, *7*(8), 1899–1914.

Rosell-Llompart, J., and J. F. de la Mora (1994), Generation of monodisperse droplets 0.3–4 micron meter in diameter from electrified cone-jets of highly conducting and viscous liquids, *J. Aerosol Sci.*, *25*(6), 1093–1119, doi:10.1016/0021-8502(94)90204-6.

Rosser, S., and J. F. de la Mora (2005), Vienna-type DMA of high resolution and high flow rate, *Aerosol Sci. Technol.*, *39*(12), 1191–1200, doi:10.1080/02786820500444820.

Saros, M. T., R. J. Weber, J. J. Marti, and P. H. McMurry (1996), Ultrafine aerosol measurement using a condensation nucleus counter with pulse height analysis, *Aerosol Sci. Technol.*, *25*(2), 200–213, doi:10.1080/02786829608965391.

Sihto, S. L., et al. (2006), Atmospheric sulphuric acid and aerosol formation: Implications from atmospheric measurements for nucleation and early growth mechanisms, *Atmos. Chem. Phys.*, *6*(12), 4079–4091.

Sipila, M., et al. (2008), Applicability of condensation particle counters to measure atmospheric clusters, *Atmos. Chem. Phys.*, *8*(14), 4049–4060.

Spracklen, D. V., et al. (2008), Contribution of particle formation to global cloud condensation nuclei concentrations, *Geophys. Res. Lett.*, *35*(6), L06808, doi:10.1029/2007GL033038.

Su, T., and M. T. Bowers (1973a), Ion-polar molecule collisions: Effect of molecular size on ion-polar molecule rate constants, *J. Am. Chem. Soc.*, *95*(23), 7609–7610, doi:10.1021/ja00804a011.

Su, T., and M. T. Bowers (1973b), Theory of ion-polar molecule collisions: Comparison with experimental charge-transfer reactions of rare-gas ions to geometric isomers of difluorobenzene and dichloroethylene, *J. Chem. Phys.*, *58*(7), 3027–3037, doi:10.1063/1.1679615.

Tammet, H. (2002), Inclined grid mobility analyzer: The plain model, paper presented at the Sixth International Aerosol Conference, Int. Aerosol Res. Assem., Taipei, Taiwan.

Turco, R. P., J. X. Zhao, and F. Q. Yu (1998), A new source of tropospheric aerosols: Ion–ion recombination, *Geophys. Res. Lett.*, *25*(5), 635–638, doi:10.1029/98GL00253.

Ude, S., and J. F. de la Mora (2005), Molecular monodisperse mobility and mass standards from electrosprays of tetra-alkyl ammonium halides, *J. Aerosol Sci.*, *36*(10), 1224–1237, doi:10.1016/j.jaerosci.2005.02.009.

Viggiano, A. A., J. V. Seeley, P. L. Mundis, J. S. Williamson, and R. A. Morris (1997), Rate constants for the reactions of $XO_3^-(H_2O)_n$ (X = C, HC, and N) and $NO_3^-(HNO_3)_n$ with H_2SO_4: Implications for atmospheric detection of H_2SO_4, *J. Phys. Chem. A*, *101*(44), 8275–8278, doi:10.1021/jp971768h.

Weber, R. J., J. J. Marti, P. H. McMurry, F. L. Eisele, D. J. Tanner, and A. Jefferson (1996), Measured atmospheric new particle formation rates: Implications for nucleation mechanisms, *Chem. Eng. Commun.*, *151*, 53–64, doi:10.1080/00986449608936541.

Weber, R. J., G. Chen, D. D. Davis, R. L. Mauldin, D. J. Tanner, F. L. Eisele, A. D. Clarke, D. C. Thornton, and A. R. Bandy (2001), Measurements of enhanced H_2SO_4 and 3–4 nm particles near a frontal cloud during the First Aerosol Characterization Experiment (ACE 1), *J. Geophys. Res.*, *106*(D20), 24107–24117.

Woo, K. S., D. R. Chen, D. Y. H. Pui, and P. H. McMurry (2001), Measurement of Atlanta aerosol size distributions: Observations of ultrafine particle events, *Aerosol Sci. Technol.*, *34*(1), 75–87, doi:10.1080/02786820130008204 9.

Young, L. H., D. R. Benson, F. R. Kameel, J. R. Pierce, H. Junninen, M. Kulmala, and S. H. Lee (2008), Laboratory studies of H_2SO_4/H_2O binary homogeneous nucleation from the SO_2+OH reaction: Evaluation of the experimental setup and preliminary results, *Atmos. Chem. Phys.*, *8*(16), 4997–5016.

Yu, F. Q., and R. P. Turco (2000), Ultrafine aerosol formation via ion-mediated nucleation, *Geophys. Res. Lett.*, *27*(6), 883–886, doi:10.1029/1999GL011151.

Yu, F. Q., and R. P. Turco (2001), From molecular clusters to nanoparticles: Role of ambient ionization in tropospheric aerosol formation, *J. Geophys. Res.*, *106*(D5), 4797–4814.

Yu, F. Q., Z. Wang, G. Luo, and R. P. Turco (2008), Ion-mediated nucleation as an important source of tropospheric aerosols, *Atmos. Chem. Phys.*, *8*(9), 2537–2554.

Zhang, R. Y., I. Suh, J. Zhao, D. Zhang, E. C. Fortner, X. X. Tie, L. T. Molina, and M. J. Molina (2004), Atmospheric new particle formation enhanced by organic acids, *Science*, *304*(5676), 1487–1490, doi:10.1126/science.1095139.

Zhao, J., and R. Y. Zhang (2004), Proton transfer reaction rate constants between hydronium ion (H_3O^+) and volatile organic compounds, *Atmos. Environ.*, *38*(14), 2177–2185, doi:10.1016/j.atmosenv.2004.01.019.

Zhao, J., A. Khalizov, R. Y. Zhang, and R. McGraw (2009), Hydrogen-bonding interaction in molecular complexes and clusters of aerosol nucleation precursors, *J. Phys. Chem. A*, *113*(4), 680–689, doi:10.1021/jp806693r.

F. L. Eisele and J. Zhao, Atmospheric Chemistry Division, National Center for Atmospheric Research, Boulder, CO 80301, USA. (jzhao@ucar.edu)

C. Kuang, Department of Chemical Engineering and Materials Science, University of Minnesota-Twin Cities, Minneapolis, MN 55455, USA.

P. H. McMurry and M. Titcombe, Department of Mechanical Engineering, University of Minnesota-Twin Cities, Minneapolis, MN 55455, USA.